

Structure and variability of the microbial community associated to the Alboran Sea frontal system (Western Mediterranean) in winter

JACQUET Stephan^{1, 2 *}, PRIEUR Louis³, NIVAL Paul³, VAULOT Daniel¹

1)- Université Pierre-et-Marie-Curie (Paris 06) and CNRS, UMR 7144, Station Biologique, BP 74, 29682 Roscoff Cedex, France

2)- INRA, Station d'Hydrobiologie Lacustre, UMR CARTELE, 74203 Thonon-les-Bains Cedex, France

3)- Laboratoire d'Océanologie de Villefranche-sur-Mer, CNRS and Université Pierre-et-Marie-Curie (Paris 6), 06234 Villefranche-sur-Mer Cedex, France

*) - Corresponding author (S. Jacquet)

E-mail address: stephan.jacquet@thonon.inra.fr

ABSTRACT: The Almofront-2 cruise (22 November 1997 – 18 January 1998) was aimed at documenting physical, chemical and biological characteristics of the Alboran Sea. Both horizontal and vertical distributions of picophytoplankton (*Prochlorococcus* spp., *Synechococcus* spp. and small photosynthetic eukaryotes), heterotrophic prokaryotes and viruses were investigated using flow cytometry (FCM). Three types of ecosystems were discriminated on the basis of physical parameters and picoplankton distribution: the Mediterranean ecosystem (MED) in the Northern part, the anticyclonic gyre of modified Atlantic (ATL) water in the southern part, and the frontal ecosystem in between. MED waters were dominated by *Prochlorococcus* while *Synechococcus* concentration was higher in ATL waters.

High concentrations of both groups were also recorded in dense waters of the front, a likely response to nutrient injection from deeper and/or adjacent waters. Photosynthetic picoeukaryotes concentration was the highest in regions influenced by the front and at the periphery of the gyre. The low biomass of picoeukaryotes in dense waters of the front suggests that this group responded very differently to environmental factors compared to *Prochlorococcus* and *Synechococcus*. Picoplankton contributed up to 50% of total chlorophyll *a* (Chl *a*) in the gyre (mean ca 25%), essentially due to the picoeukaryotes.

The biomass of the picophytoplankton clearly decreased between the two legs. Heterotrophic bacteria concentrations were well correlated to those of picoeukaryotes and reached their maximum in the central part of the Alboran eastern gyre. Two patches of high concentration of heterotrophic bacteria were recorded in frontal-influenced MED waters and were tightly coupled to maximal Chl *a* concentrations following the 28.1-28.2 density excess isolines. At this period of the year, picoplankton could represent up to 50% of the <200 µm living organic carbon in MED waters and up to 35% in modified ATL waters (mean 35 and 23%, respectively). At last, two groups of virus-like particles (VLPs) were discriminated by FCM according to DNA content fluorescence. No major differences in their distribution patterns were recorded between sites. A significant correlation was found between heterotrophic bacteria numbers and VLPs suggesting a tight coupling between the two communities. In

conclusion, picoplankton appears to constitute an important fraction of living matter in the Alboran Sea at the end of fall and early winter and may thus participate significantly to carbon and energy fluxes in the W. Mediterranean Sea.

KEY WORDS:

Alboran sea, frontal structures, picoplankton, virus, microbial communities, carbon biomass.

ACRONYMS

CTD: conductivity, temperature, depth sensors

FCM: flow cytrometer

DML: Depth of mixed layer, DCM: Deep chlorophyll maximum

ATL: Atlantic waters, MAW: Modified Atlantic Water; MED: Mediterranean waters,

LIV: Levantine intermediate water

VLP: virus like particles

Introduction

Hydrological fronts are mesoscale structures, characterized by an important horizontal gradient of salinity and temperature, where physical and biological processes interact with each other. An important characteristic of frontal-jet systems is that the main water mass circulation is not exactly in geostrophic balance. Such small unbalance generates secondary circulations, both horizontally and vertically (Bower & Rossby, 1989) and localized vertical velocities that may be responsible for nutrient enrichment in the mixed layer from adjacent or upwelled waters (Fasham *et al.*, 1985). Hence, frontal structures in the ocean constitute a dominant source of phytoplankton heterogeneity and biomass enhancement (Franks, 1992). Rodriguez *et al.* (2001) proposed that the response of phytoplankton can vary with its size structure that may depend more on hydrodynamics than nutrients in frontal ecosystems, while some authors reported that, in a frontal structure, the combination of nutrients and light levels are likely to be the main responsible for both the biomass enhancement and community structure of the phytoplankton (Claustre *et al.*, 1994).

In the Alboran Sea, surface Atlantic waters enter the Mediterranean Sea through the strait of Gibraltar. Strong interactions occur between this flow (referred to as the Atlantic jet) and local Mediterranean waters resulting in the geostrophic Almeria (Spain) - Oran (Algeria) frontal jet surrounding an anticyclonic eddy (Cheney & Doblar, 1982; Farmer & Armi, 1988; Tintoré *et al.*, 1988). The nutrient-enriched Atlantic inflow has been reported to enhance primary production of Mediterranean waters (Gould & Wiesenburg, 1990; Minas *et al.*, 1991). During the Almofront-1 cruise (held in spring 1991), primary production was reported to be 2.5 higher in the frontal zone compared to surrounding waters, essentially due to diatoms (Prieur & Sournia, 1994). Nutrient availability in adjacent waters and an important secondary circulation at the basis of the euphotic zone were shown to be responsible of the frontal fertilization in an environment where surrounding waters remained relatively oligotrophic (Prieur *et al.*, 1993).

Marine microbial communities are an important part of the pelagic ecosystem and food web (Azam *et al.*, 1983; Thingstad *et al.*, 1997). For nearly two decades, numerous laboratory and field studies focused on the ecology of picoplankton (organisms < 3µm in size) revealing the great importance of the picophytoplankton in the global carbon fixation in marine systems (Marañón *et al.*, 2001). The cyanobacterium *Prochlorococcus*, the most abundant photosynthetic organism on Earth, is widely distributed both horizontally (between 40°N and 40°S) and vertically (over the whole euphotic zone), with maximum concentrations exceeding 10⁵ cell.ml⁻¹ (reviewed in Partensky *et al.*, 1999; West & Scanlan, 1999). It is mostly associated to oligotrophic and well-stratified provinces of the ocean where it contributes significantly to the primary production (Campbell *et al.*, 1994; Li, 1994). The cyanobacterium *Synechococcus* is more widespread since it is less sensitive to temperature than

Prochlorococcus and accommodates to a larger range of trophic status and water column mixing conditions (e.g. Partensky *et al.*, 1999) although it is generally restricted to the upper well-lit layer. Compared to *Prochlorococcus*, its concentration is usually lower in the range 10^4 - 10^5 cell.ml⁻¹ and decreases even further in oligotrophic waters. Distribution of photosynthetic picoeukaryotes is less documented than those of photosynthetic prokaryotes because, in contrast to the latter, flow cytometry does not allow identifying their taxonomy on the basis of their sole fluorescence and scatter signatures except for orange-fluorescing cryptophytes. In recent years, however, the use of molecular approaches has permitted to establish the major picoeukaryote taxonomic groups present in marine waters (reviewed in Vaultot *et al.*, 2008; Worden & Not, 2008), including the Mediterranean sea (Díez *et al.*, 2001; Marie *et al.*, 2006; Viprey *et al.*, 2008) which include Prasinophyceae, Haptophyta, and Chrysophyceae. Picoeukaryote concentrations reach typically 10^3 cell.ml⁻¹. Heterotrophic bacteria constitute a very diversified community (Torsvik *et al.*, 2002). Although these cells colonize the whole water column, their highest concentrations are recorded in the euphotic layer with typically 10^5 to 10^6 cell.ml⁻¹ (reviewed in Ducklow, 1999). Viruses have been recently recognized as the most abundant biological particles in the sea with concentration reaching up to 10^8 viruses.ml⁻¹ (Bergh *et al.*, 1989; Wommack & Colwell, 2000; Suttle, 2007). Although they participate only weakly to the carbon stock, they may have important roles in the genetic control of host diversity and the transfer of organic matter directly from auto- and heterotrophic communities to dissolved organic matter (reviewed in Fuhrman, 1999; Wilhelm & Suttle, 1999; Middelboe, 2008; Jacquet *et al.*, 2010).

We participated to the Almofront-2 cruise which took place in late 1997-early 1998. We documented these biological compartments from a large set of samples analyzed by flow cytometry. Our main goal was to document the coupling of picoplankton and virus-like particles with biological, chemical or physical processes in a region characterized by strong hydrological and trophic situations.

Materials and methods

Sample collection

The Almofront-2 cruise held in the Alboran Sea (Western Mediterranean Sea). Sampling took place in the eastern part of the Alboran Sea, between 0° and 3°W longitude and between 35° and 37°N latitude (Fig. 1). During leg-1 of the cruise (1st – 21th December 1997), one north-south transect was sampled at 24 stations during 3 days (referred to as CTD 252 to 275) separated from each other by about 3 nautical miles (see Cuttelod & Claustre, 2010) when crossing the frontal jet – gyre system, 5 miles otherwise. In the rest of the text, we will refer to stations or CTD as synonymous terms. This transect was designed to obtain a general description of the whole area and to localize precisely the jet-front-gyre system. Twelve depths between 0 and 200 m were sampled for each station. During leg-2 (23 December 1997 – 15 January 1998), 8 representative sites of the range of hydrodynamical and biogeochemical situations encountered during leg-1, were occupied for a period of 36 h and sampled between 8 and 10 times (Fig. 1). For each site, we selected 3 different profiles between 0 and 200 m depth every 12 h (at general around 8:00 and 20:00 the first day and 8:00 the second day, local time) to document the picophytoplanktonic fraction plus 1 profile describing the entire water column, from surface to bottom (20:00), to obtain counts of both heterotrophic bacteria and virus-like particles. From 12 to 18 samples were taken for each CTD profile using 10L-Niskin bottles from an oceanic CTD Rosette (SEABIRD SBE32, Seattle, USA). The CTD was equipped with a SEABIRD O2 probe (SBE911+and rosette, Seattle), a CHELSEA fluorometer (Aquatracka III, U. K.), a SEA-TECH transmissiometer (Corvallis, USA) and two sensors for PAR (Photosynthetic Active Radiation, ref. QSPL2/4S) and SPAR (Surface Photosynthetic Active Radiation, ref. QSR 240) measurements (Biospherical Inst., San Diego, USA).

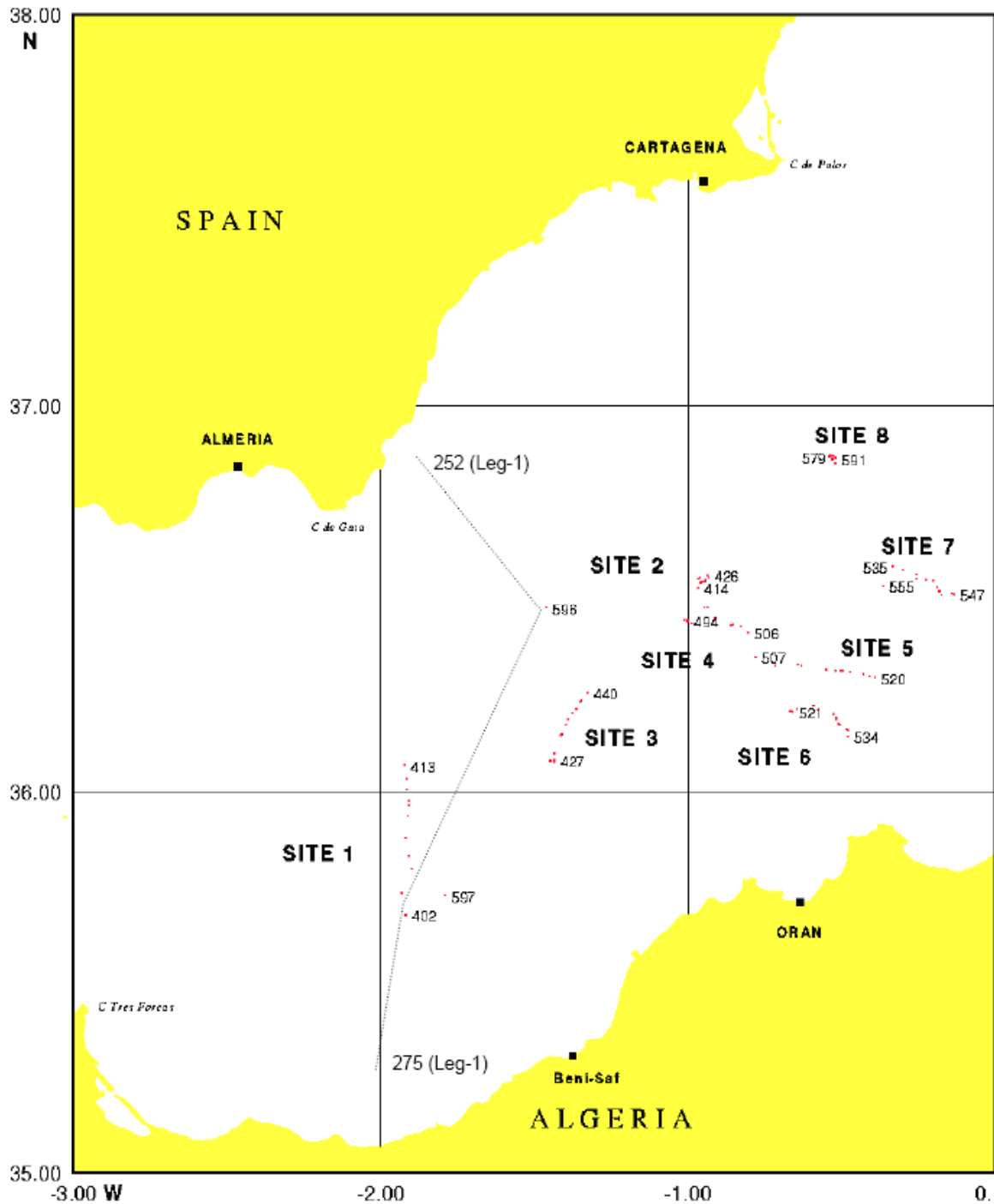


Figure 1 : Sampling locations of the Almofront-2 cruise in the Alboran Sea (SW Mediterranean Sea).

During the first leg of the cruise, a north-south transect was intensively sampled as symbolized by dashed lines. The 24 stations referred to as CTD 252 to 275 (see Cuttelod & Claustre, 2010) were separated from each other by about 5 nautical miles but CTD 260 to 269 by 3 n. miles and sampling was performed over the 0-200 m water column at 12 different depths.

During the second leg, 8 sites characterized by several stations were occupied for 36 h near the drift of the sediment trap line (0-400 m) deployed at starting time of each site. Both the photic and the aphotic layers were sampled in ‘Mediterranean waters’ (sites 2, 8), the front (site 7), the Atlantic baroclinic jet (sites 1, 4, 5) and the eastern Alboran gyre (sites 3, 6).

Sample processing

Samples were fixed during the cruise using a mixture of glutaraldehyde and paraformaldehyde (0.05 and 1% final concentration respectively) for 20 min and immediately frozen in liquid nitrogen (see Jacquet *et al.*, 1998). Back to the laboratory, samples were stored at -80°C . Prior to analysis, samples were rapidly thawed at 37°C and divided into two aliquots: one for natural fluorescence analysis to get counts of autotrophic population, the other to enumerate heterotrophic bacteria after 10 min incubation of the samples with the fluorescent nucleic acid dye SYBRTMGreen I (Molecular Probes, 1/10,000 final concentration, Marie *et al.*, 1997). Samples collected during the surface to bottom profile were divided into 3 aliquots, the last one being used to estimate titers of virus-like particles according to Marie *et al.* (1999). Briefly, samples were diluted from 1:5 to 1:10 in TE buffer (Tris 10 mM, EDTA 1 mM, pH 7.5), then incubated with SYBRTMGreen I at a final concentration of 1/20,000 for 15 min in subdued light.

Flow cytometric analysis and data processing

Samples were analyzed with a FACSortTM flow cytometer (FCM, Becton Dickinson, San Jose, CA). Setup for natural fluorescence was as previously described (Partensky *et al.*, 1996). *Prochlorococcus* had low red chlorophyll fluorescence and could be easily discriminated from both the photosynthetic picoeukaryotes community and the background noise (Fig. 2A, B). *Prochlorococcus* and photosynthetic picoeukaryotes were discriminated from *Synechococcus* cyanobacteria on the basis of the orange phycoerythrin fluorescence of the latter (Fig. 2B). On stained samples, both photosynthetic picoeukaryotes and *Synechococcus* could be discriminated from other bacteria because of their higher red chlorophyll fluorescence (Fig. 2C). It was not the case for *Prochlorococcus* because of dim red fluorescence of the cells (Fig. 2C). Because, when stained, the two communities of *Prochlorococcus* and heterotrophic bacteria could not be discriminated by flow cytometry, the actual abundance of heterotrophic bacteria was determined by subtracting the *Prochlorococcus* concentration determined on non-stained samples from the sum of the two populations obtained on stained samples. Two groups of virus-like particles referred to as V-I and V-II, following Marie *et al.* (1999), were discriminated according to the green dye-DNA fluorescence *vs.* right angle scatter (Fig. 2D). 0.95 μm fluorescent beads (Polyscience) were added to all samples and FCM parameters were normalized to them. Data were collected on “listmode files” and then analyzed using CYTOWIN (Vaulot, 1989, available freely at <http://www.sb-roscoff.fr/Phyto/>).

Confocal microscopy analysis

Confocal Laser Scanning Microscopy (CLSM, Fluoview, Olympus Optical Co., Tokyo, Japan) and image analysis were used to estimate the size of heterotrophic bacteria (Jacquet *et al.*, 2002). Several samples from different depths and different hydrological situations were filtered onto 0.2 μm pore size inorganic membrane filters (Anodisc, WhatmanTM, Maidstone, UK). The filter disk was placed onto a slide. A 20 μl mixture (50%-50%) of normal PBS (Phosphate Buffer Saline, Sigma, Saint-Quentin Fallavier, France) and bi-distilled glycerol ($d=1.26$, Fisher scientific, Elancourt, France) was added with a drop of SYBRTMGreen I (1/1,000 final concentration). A 22 x 40 mm coverslip was overlaid on preparation. Images were acquired with the Fluoview software and processed using Image Tools. The average size (i.e. spherical equivalent) of bacteria was found to be 0.48 μm (SD=0.14, n=194).

Carbon biomass estimation

For heterotrophic bacteria, we used a conversion factor of 20 $\text{fgC}\cdot\text{cell}^{-1}$ (Lee & Fuhrman, 1987) that appears appropriate for cells ranging between 0.4 and 0.5 μm in diameter. Typical JGOFS values were used for the other groups, i.e. 53 $\text{fgC}\cdot\text{cell}^{-1}$ for *Prochlorococcus*, 250 $\text{fgC}\cdot\text{cell}^{-1}$ for *Synechococcus* and 2,108 $\text{fgC}\cdot\text{cell}^{-1}$ for photosynthetic picoeukaryotes (see Campbell *et al.*, 1994 and references therein). To integrate carbon biomass through the water column, a uniform depth of 100 m was chosen rather than the mixed layer (that could vary between stations) or the euphotic zone (since low cell concentrations were often recorded below 60-70 m, i.e. the depth of 1% light). For viruses, we used 0.08 $\text{fgC}\cdot\text{particle}^{-1}$, according to Bratbak *et al.* (1992).

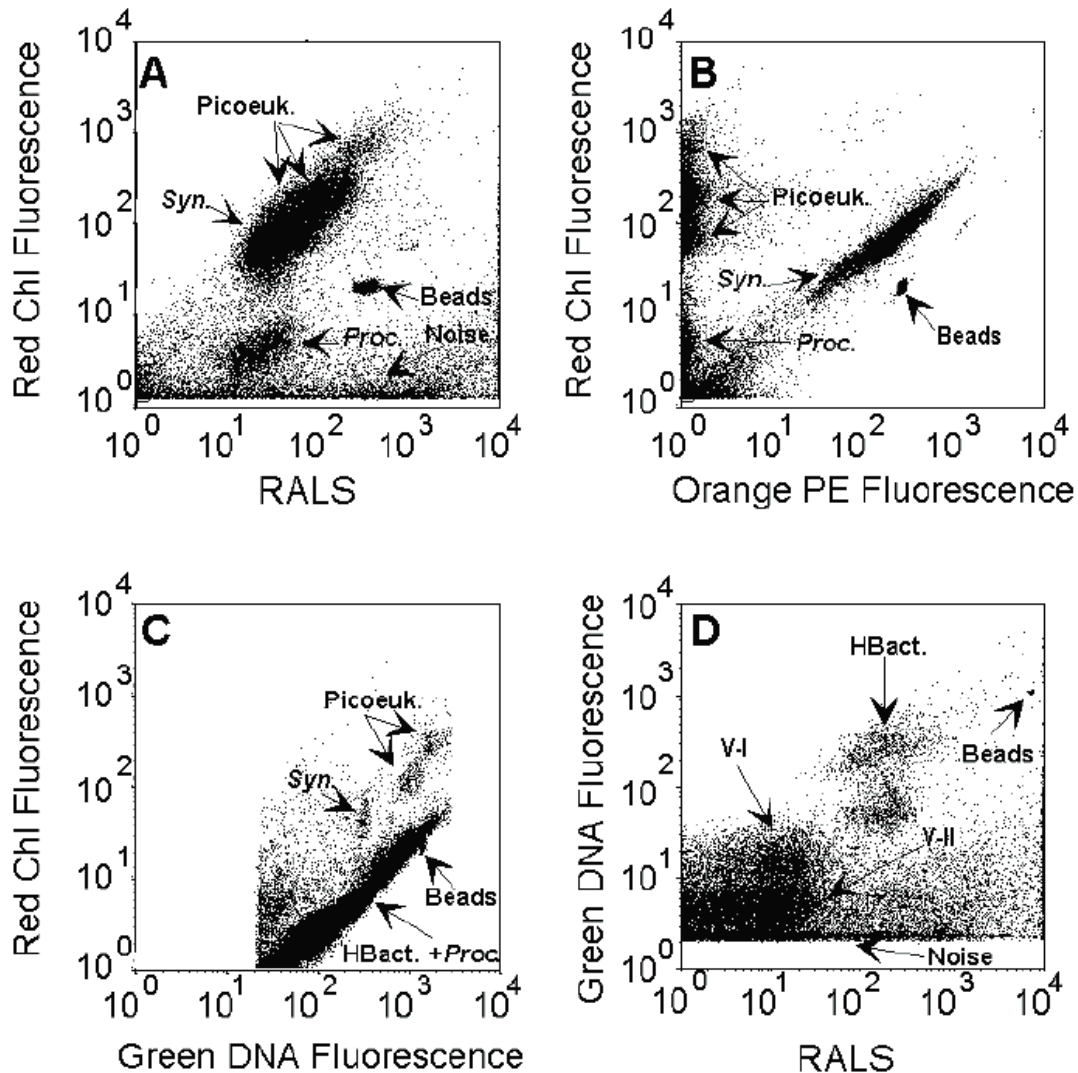


Figure 2 : Flow cytometric analysis of natural populations sampled in the Alboran Sea. Prochlorococcus, Synechococcus and picoeukaryotes were discriminated on the basis of their right angle light scatter (RALS) vs. their red chlorophyll fluorescence (A) or phycoerythrin orange fluorescence (B) from unstained samples. Heterotrophic bacterial populations were discriminated on the green DNA fluorescence vs. red fluorescence (C) and RALS (D) from SYBR Green stained samples. Viruses referred to as V-I and V-II (D) were discriminated on the basis of the green DNA-dye complex fluorescence vs. their RALS.

Other data sets

Density and chlorophyll fluorescence profiles were obtained from CTD instrumentation that measured these parameters continuously (see figures 3, 4). Density excess (kg.m^{-3}) was obtained from UNESCO standard equations. Chlorophyll *a* fluorescence was measured with the Chelsea fluorometer and converted to biomass (mg.m^{-3}) using appropriate conversion factor (i.e. $1.85 \times F$ according to Cuttelod & Claustre, 2010). Horizontal current profiles was acquired with 2 ADCP 75 and 300 kHz vessel-mounted RDI[®] Acoustic Doppler Current Profiler (ADCP results shown in Sempéré *et al.*, 2003). Measurements of inorganic nutrient concentrations (nitrate, nitrite, phosphate) were carried out using a Technicon AutoAnalyser II according to standard colorimetric methods and following the procedures given in Tréguer & Le Corre (1975).

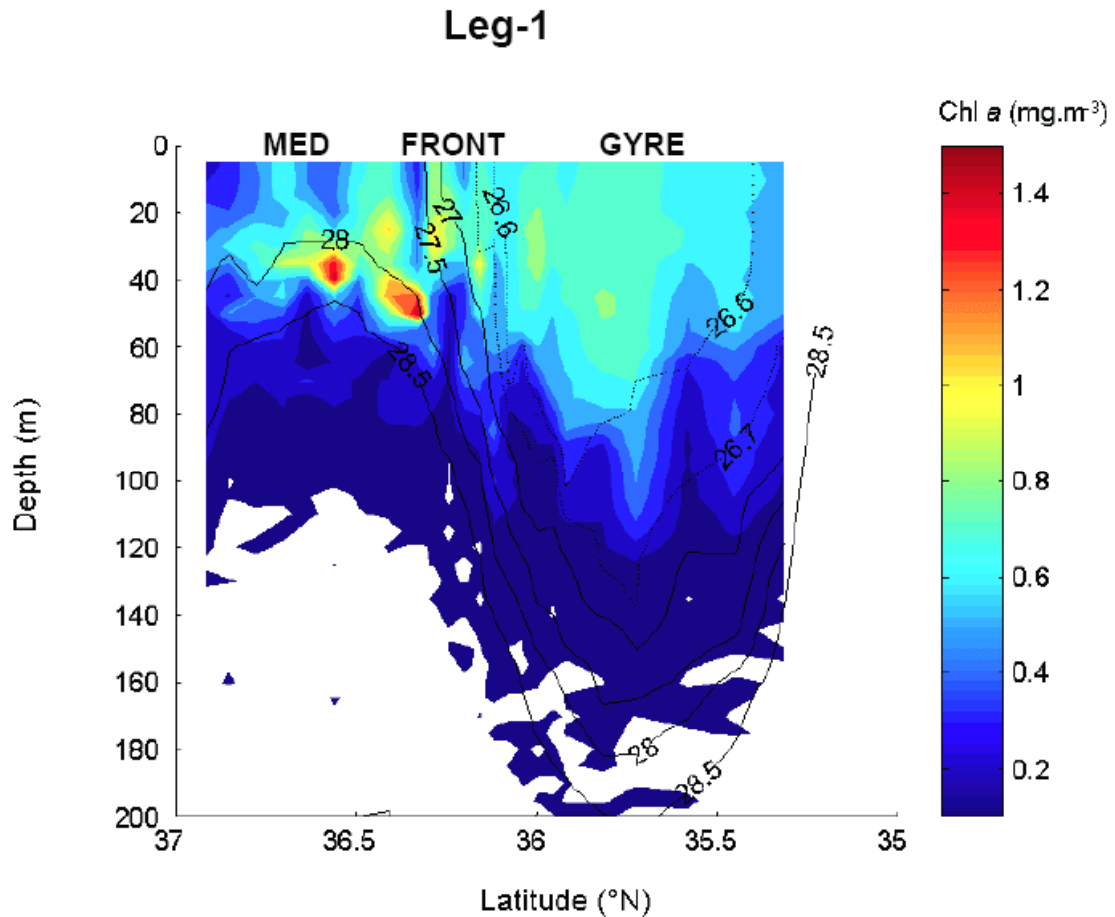


Figure 3 : Density profiles (kg.m⁻³) and chlorophyll *a* distribution (mg.m⁻³) along the CTD 252- 270 transect of leg-1 of the Almofront-2 cruise (between 13 and 16 December 1997).

Results

Hydrological conditions and chlorophyll distribution

Surface Atlantic water flowing into the Mediterranean Sea does not mix immediately with Mediterranean waters but their characteristics change progressively to the modified Atlantic waters (MAW) which are found in the western Mediterranean basin.

The North South transect crossed three types of hydrological structure (*leg 1*) :

(1) the Mediterranean waters (MED), cold and very saline, could be divided into two types referred to as MED-1 waters (CTD 252 to 255) from the Spanish coastal current that originated from the North Mediterranean and, more to the south, MED-2 waters (CTD 255 to 259, Conductivity, Temperature, Depth profiles are here the name of sampling stations);

(2) the Atlantic jet, the maximum current speed being found at CTD 260 to 268. The frontal structure was located between CTD 260 and 263, the gradient of temperature and salinity being particularly clear in surface waters at CTD 260 and 261. The core of the jet, as revealed by maximum current speed (up to 80 cm.s⁻¹), correspond to CTD 264 and 265 (see Fig. 3 in Sempere *et al.*, 2003).

(3) the Eastern Alboran anticyclonic gyre was revealed by surface warm water and density profiles with a deep mixed layer (CTD 269 to 275). The central part of the gyre for which current speed is weak, is sampled by CTD 271-272.

The bottom depth of surface mixed layer shifted from 30-40 m to about 110-130 m between the dense MED waters and the central part of the gyre. The maximum of Chl *a* concentration was tightly coupled to the 28.1–28.2 density excess isolines with two important patches ($>1.2 \text{ mg}\cdot\text{m}^{-3}$) recorded in MED-2 waters and in the dense waters near the front between 30 and 50 m (Fig. 3). In surface waters, significant concentrations of Chl *a* were mostly recorded in Atlantic and frontal influenced waters.

During the second leg, a well-stratified water column with excess density close to 28.0 ($S>37.5$ and $T<16^\circ\text{C}$) and a 25 m deep surface mixed water characterized MED waters at sites 2 and 8 (Fig. 4 A, B).

In contrast, the water column profile in the frontal structure (site 7 corresponding to both the left side of the jet in surface and to MED waters at depth, see Fig 5) was more heterogeneous (Fig. 4C). A clear stratification was observed at the depth of 10-15 m, followed by a constant increase of density with depth until 100 m. However, two discontinuities in both temperature and salinity occurred between 15 and 60 m and between 60 and 100 m, respectively. An important Chl *a* maximum was recorded between 20 and 30 m (Fig. 4). However the amplitude and depth position of the maximum is changing between the 3 casts shown although small distance between these casts. The two first casts exhibit the strongest maxima, the third few hours after, with a deeper maxima around 40-50 m depths. It could be noted that the Chl *a* remains noticeable near 70-80 m depths ($S>28.2$) although inside the Med waters below the surface jet flow of MAW.

Closer to the jet core, but always on its left side looking downstream, the water column was homogenous over the first 30 m and a broad pycnocline developed between 30 and 150 m (site 4, Fig. 4D). Only weak variation in the profile structure between the 2 first relevant stations of site 4 and a Chl *a* fluorescence was recorded constant in mixed layer and weak at below depths. The third station exhibits a 50 m mixed layer and abrupt change in Chl *a* below, so during this site exploration the mixed layer increase the depth of mixed layer at constant Chl *a* concentration in.

In the core of the jet where surface current velocity was the highest (site 5), water column was homogeneous over the first 50-70 m and the pycnocline began at 80 m (Fig. 4E). The concentration of chlorophyll is constant from surface to 80 m although some variation occurs at the bottom of mixed layer.

The right side of the jet sampled at site 1 was characterized by a constant vertical gradient in density, temperature and salinity, between 30-45 m and 150 m and by a contrasted profile in Chl *a* with a minimum at 60 m and a strong maximum at 80 m for two among three profiles (Fig. 4F).

A well-mixed water column over the first 100 m characterized the outer side of the Alboran eastern gyre (site 6) with weak deep maximum for one among the 3 profiles of this site. Finally, near the centre of the gyre (site 3), the water column was well mixed over 80-100 m (Fig. 4G, H). The chlorophyll concentration was constant in the mixed water column and there was no deep maximum Chl *a* fluorescence at these two sites.

Other relevant characteristics recorded during leg-2, i.e. depths of the mixed layer (DML) and of chlorophyll maximum (DCM), as well as concentrations in inorganic nutrients in surface and at DCM are reported in Table 1.

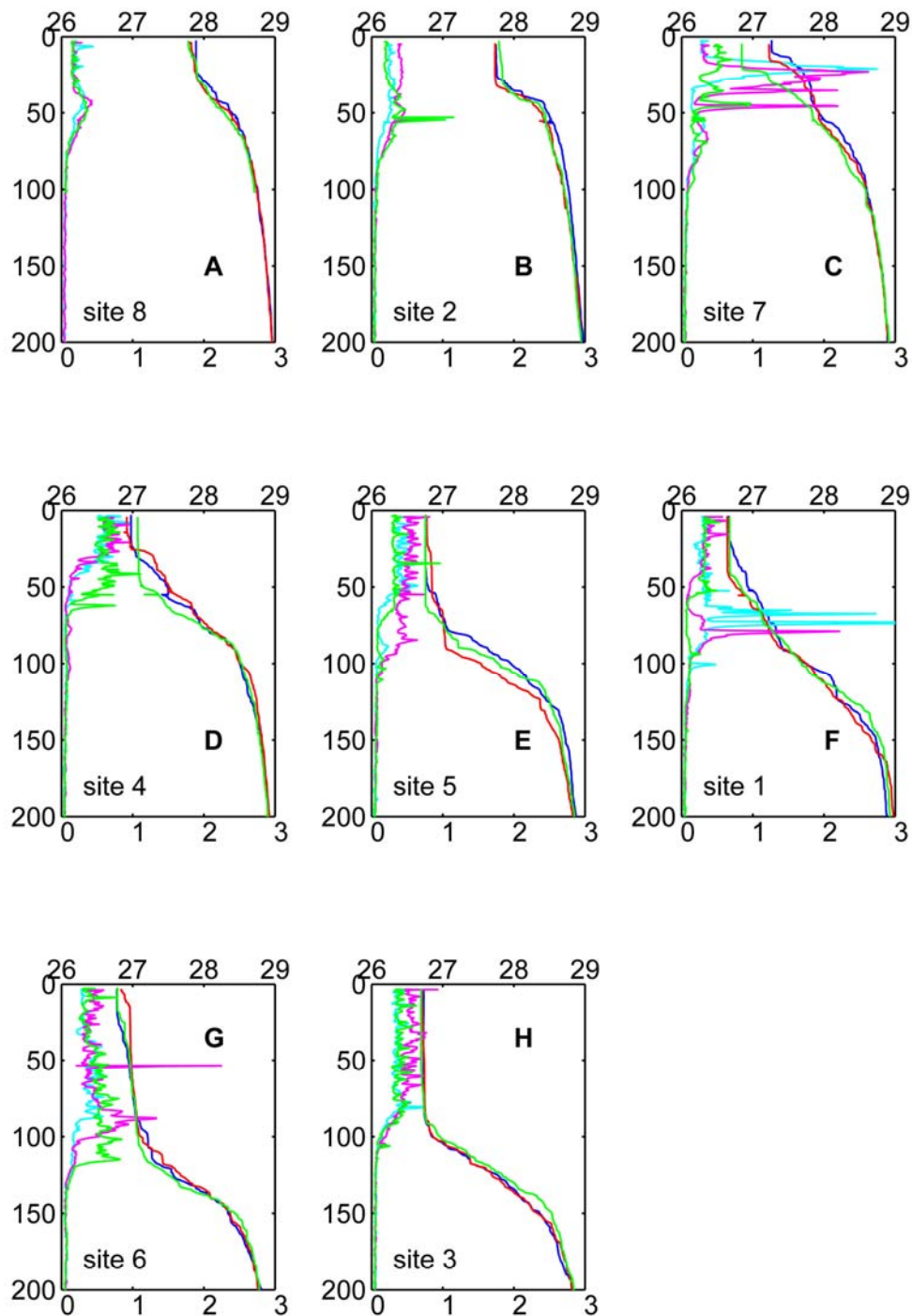


Figure 4. Density excess (26 to 29 kg.m⁻³) and chlorophyll a calibrated fluorescence (1 to 3 mg.m⁻³) vertical profiles recorded at 3 selected stations for each of the 8 sites investigated during leg-2 of Almofront-2 cruise. Blue, red and green color line respectively stands for the 1st, 2nd and 3rd density profiles listed in table 1, and corresponding Chl *a* color are cyan, mauve and green.

Microbial community in Alboran sea frontal system

Table 1: Hydrographical characteristics of the 3 selected stations per site during leg 2:

Site number;

Stations: (CTD numbers) ;

Latitude;

Longitude;

DML : depth of the mixed layer (m);

DCM : depth of the chlorophyll *a* fluorescence maximum (m);

Concentration of nitrates (N-NO₃), nitrites (N-NO₂), phosphates (P-P₀₄) at surface and DCM (μM).

Site	CTD #	Lat. (°N)	Long. (°W)	DML (m)	DCM (m)	NO ₃ _{surf} (μM)	NO ₃ _{DCM} (μM)	NO ₂ _{surf} (μM)	NO ₂ _{DCM} (μM)	PO ₄ _{surf} (μM)	PO ₄ _{DCM} (μM)
8	581	36.861	0.529	50	25	0.06	2.73	0.01	0.14	0.01	0.07
	584	36.849	0.520	47	30	0.03	3.04	0.01	0.11	0.00	0.05
	588-7	36.871	0.535	50	30	0.03	1.78	0.00	0.17	0.00	0.02
2	416	36.542	0.958	42	35	0.06	3.20	0.02	0.12	0.00	0.04
	419	36.554	0.959	45	35	0.06	2.48	0.01	0.15	0.00	0.04
	423-2	36.543	0.943	45	32.5	0.06	2.35	0.00	0.17	0.00	0.04
7	537	36.584	0.333	40	15	0.24	1.37	0.02	0.09	0.00	0.03
	540	36.562	0.256	37	17	0.12	0.76	0.02	0.06	0.00	0.01
	544-3	36.519	0.181	35	22	0.09	0.09	0.02	0.02	0.00	0.00
4	496	36.438	1.001	47	28	0.37	0.37	0.08	0.08	0.00	0.00
	499	36.475	0.937	37	26	0.43	0.43	0.11	0.11	0.01	0.01
	503-2	36.430	0.857	67	50	1.01	1.22	0.09	0.10	0.02	0.02
5	509	36.346	0.78	72	55	0.56	0.56	0.21	0.31	0.01	0.01
	512	36.325	0.632	62	42	0.51	0.51	0.23	0.23	0.01	0.01
	516-5	36.311	0.502	82	65	0.64	0.64	0.25	0.25	0.01	0.01
1	403	35.667	1.917	40	35	0.77	1.05	0.35	0.09	0.03	0.02
	406	35.831	1.906	60	42	0.80	0.71	0.36	0.09	0.04	0.02
	410-9	35.962	1.909	57	40	0.78	0.78	0.28	0.27	0.02	0.01
6	523	36.206	0.66	55	30/80	0.53	0.31	0.32	0.25	0.02	0.04
	526	36.212	0.573	42	25/80	0.43	0.65	0.25	0.29	0.02	0.03
	530-1	36.175	0.507	50	30/90	0.55	1.4	0.33	0.30	0.02	0.05
3	429	36.078	1.417	110	100	0.78	0.78	0.27	0.27	0.01	0.01
	432	36.140	1.411	92	100	0.74	0.74	0.27	0.27	0.04	0.05
	436-5	36.200	1.375	100	97	0.71	0.8	0.34	0.32	0.01	0.02

3.2. Comparison between legs

Characteristics and positions of stations (leg-1) and sites (leg-2) were compared based on density profiles, ADCP measurements and GPS data (Global Positioning System). The meander-gyre system clearly moved eastwards during the second leg (about 56 miles between 22 December and 16 January, see VanWambeke, 2004), so that geographical positions did not correspond to the same water masses at any period of time throughout the period of study. Nevertheless, vertical profiles sampled during leg-2 could be compared to those obtained on the north-south transect of leg 1 (Table 2). It has to be noted that the initial location of each site was chosen after a 12 hours survey at 12 knots as for Almofront 1 cruise (Prieur & Sournia, 1994; Claustre *et al.*, 2000) in order to follow this slow North Eastwards drift of the whole frontal jet –eddy structure using real time information from ADCP profiles and Thermosalinograph. Therefore the long-time stations can be referred to one of the typical situation observed along the North-South transect of leg 1. They illustrate as a virtual frontal system (Fig 5), the real one which is in Alboran basin continuously stretching or compressing under the effect of the large scale forcing factors.

Table 2: Correspondence between sites from Leg 2 and stations from Leg 1 transect. Sites are ranked as to follow the North-South structure observed in the transect. Stations are named by the CTD number.

Sites (Leg 2)	Stations (Leg 1)	Characteristics
2	259-263	Mediterranean (MED2) waters
8	258-259	Mediterranean (MED 2) waters
7	260-262	Left side of the jet near surface front meander crest
4	262-263	Left side of jet core (south-eastward current)
1	262-263	Right side of jet (northward current, meander through)
5	264-265	Right side of jet core (south-eastward current)
3	266-267	Eddy (weak northward current)
6	266-267	Eddy (weak north-easterly current)

Mediterranean sites 2 and 8 show the same density profiles than MED-2 waters in leg 1's transect. Sites 7, 4, 5 are representative of the frontal gradient structure. Site 4 and 7 represent the left side of the jet. More precisely, the first day spent at site 7 could be related to the left side of the jet whereas the second day was more towards the core part of the jet. The current direction (south-eastward) suggests the site 7 is on the eastern part of the meander crest of the frontal jet-eddy system. Site 5 was a southeast current is also observed is similar to the right side of the jet core. Site 1 is typical of a frontal structure but the northward current indicate that it is in the western part of the front-eddy system and near the through of the jet meander.

The anticyclonic gyre with a weak Atlantic water mixed layer stratification is sampled by site 6 with a southeast current in surface, and site 3 where a weak north-eastwards current was observed. The position of the successive CTD profiles, made at each site on the drifting ship by following the sediment trap drifting line, illustrate the current pattern in this part of Alboran Sea (Fig 1).

So, by relocating the leg2 sites in a moving frame (Fig. 5) of the frontal jet-gyre system and using physical properties (density, mixed layer depth, horizontal currents) and Chl *a*, it is straightforward to compare how the bacterial communities change or not between the leg 1 and leg 2 cruise (Table 2). By comparing Chl *a* section of figure 3 and profiles obtained at each sites (Fig. 4) it easy to confirm that the repartition horizontal and vertical of Chl *a* were similar. In addition the intra-site variability between profiles were already proved much below the inter-site variability on physical properties (Van Wambeke *et al.*, 2004), suggesting that physical and hydrodynamical forcing drive the biomass distribution through the system, despite of its North eastwards drift.

Table 3: Characteristics of the mixed upper layer at the different sites in Leg 2. Depth of the homogeneous layer (Z) for water density and picoplankton cells abundance.

Sites	Types	Z- Excess density (m)	Z- Prochlorococcus (m)	Z- Synechococcus (m)	Z- picoeucaryotes (m)
8	Med	25	40	30	20
2	Med	30	30	25	20
7	Front outside jet	15	20	10	10
4	Front inside jet	25	20	25	20
5	Jet	55	70	70	70
1	Jet	45	50	35	40
6	Gyre border	gradient	110	gradient	110
3	Gyre center	90	90	90	100

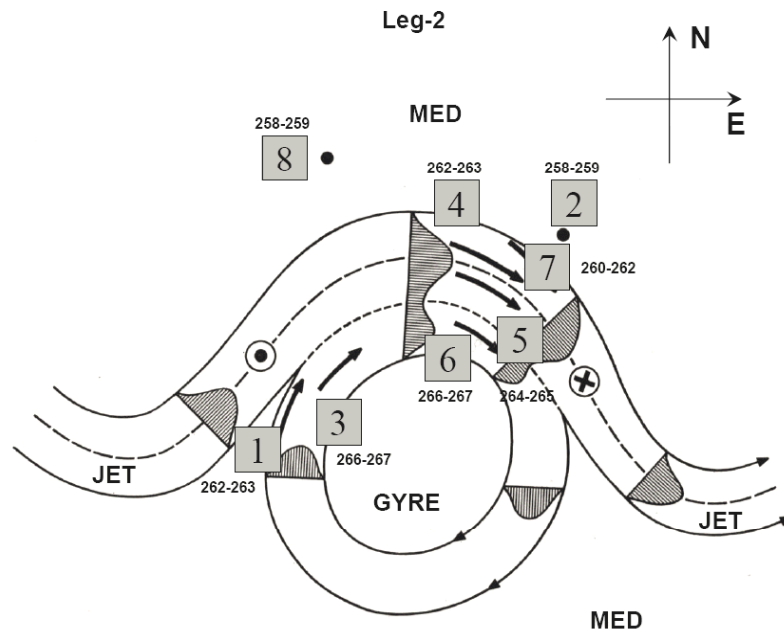


Figure 5: Schematic positions of sites in a moving frame of the jet-front-gyre system explored during leg-2.

Arrows symbolize horizontal current strength of the horizontal flow in different parts of the meandering frontal jet – gyre structure, as measured by ADCP.

In addition, a circle point and a cross are set near the curved axis of the meandering jet to symbolize some upward (circle point) and downward flow (cross) currently observed in such system (Bower & Rossby, 1989). However other kind of secondary circulations, involving vertical velocities and transverse to frontal system, are possible at submesoscale as suggested in text and by Prieur et al.(1993) or Klein and Lapeyre (2009).

Structure of the microbial communities

North South transect (Leg 1)

Along the transect *Prochlorococcus* cells were more abundant in Mediterranean waters (MED1, $6.3 \cdot 10^3 \cdot \text{ml}^{-1}$) than in the gyre waters (Fig. 6A). They are relatively abundant in the north side of the front. More south, abundances are low and similar in the jet and in the centre of the gyre ($31 \cdot 10^3 \cdot \text{cells ml}^{-1}$).

Synechococcus displayed the same spatial trend as *Prochlorococcus* in the north part of the transect (max in MED1, $40 \cdot 10^3 \cdot \text{ml}^{-1}$) (Fig. 6B), except a more rapid decrease of abundance with depth. In contrast to *Prochlorococcus*, *Synechococcus* concentrations are relatively abundant ($45 \cdot 10^3 \cdot \text{ml}^{-1}$) in the jet and inside the gyre.

Photosynthetic picoeukayotes concentration is relatively low in MED waters ($1 \cdot 10^3 \cdot \text{ml}^{-1}$). These cells were abundant in the frontal waters where *Prochlorococcus* and *Synechococcus* were relatively less abundant than in other places. The highest concentration was recorded in the centre of the gyre ($23 \cdot 10^3 \cdot \text{cells ml}^{-1}$) and the high concentrations layer extend deeper. The spatial distribution of these cells appears to follow the isopycnal distribution

Heterotrophic bacteria show an increasing concentration from north to south (Fig. 6 D) High concentrations are found in the gyre core where their pattern appears to be shaped by the density pattern, as for picoeukaryotes. In the Northern part of the transect the low abundance of heterotrophic bacteria in the MED 1 waters but quite high concentration in MED 2 waters contrasts with the *Prochlorococcus* and *Synechococcus* abundances. Spots of high concentrations are found at the depth of 30 m in MED 2 water and deeper in the front (50 m).

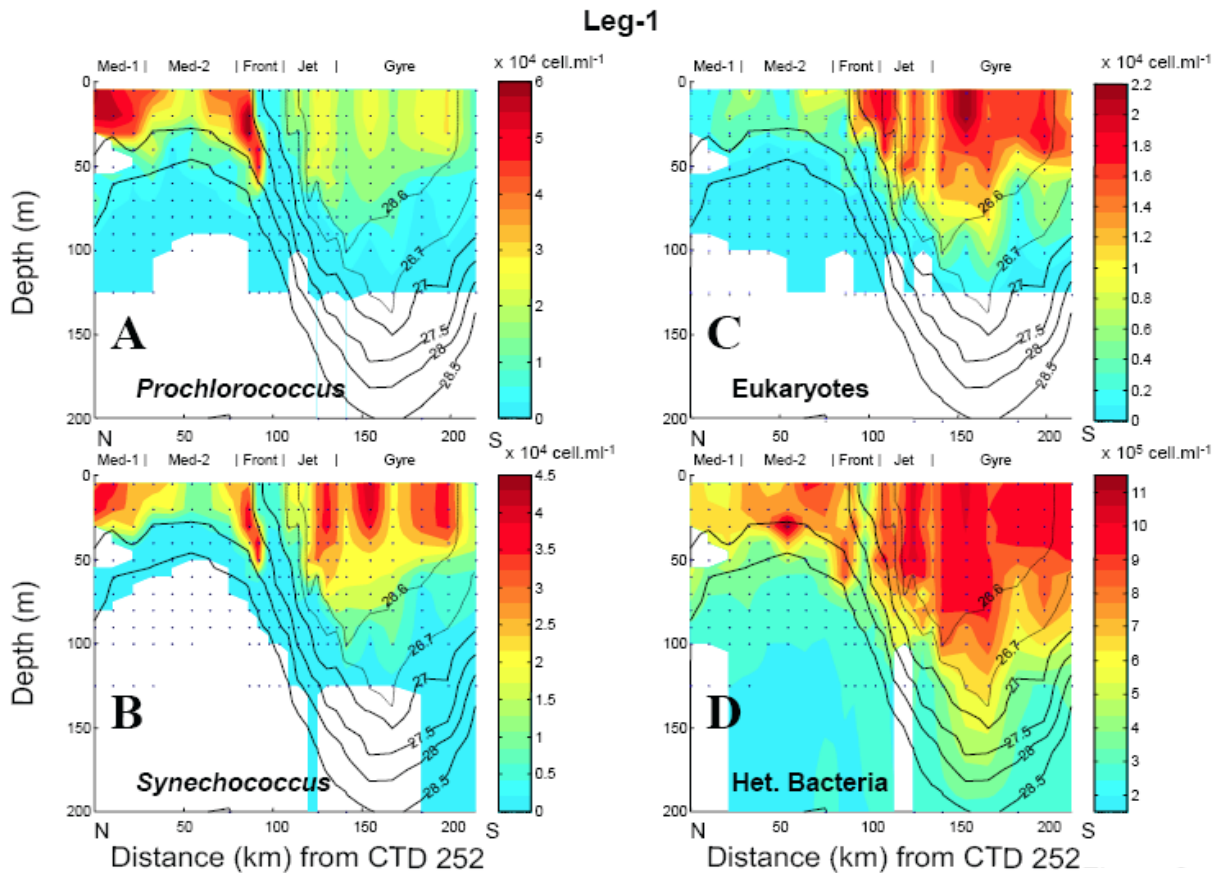


Figure 6 : Distribution of picoplanktonic populations along the transect 2 of leg-1 of the Almofront-2 cruise. (A) *Prochlorococcus*, (B) *Synechococcus*, (C) picoeukaryotes, (D) heterotrophic bacteria. Distances are given in km from CTD 252 (North). Density isolines are expressed in kg.m $^{-3}$. Note that the color scale varies with groups.

A common pattern to all groups (except *Prochlorococcus*) is a relatively high abundance in the deep water in the gyre, reaching 100 m which suggest there a downwelling effect. Nevertheless the higher abundance in surface water might be the consequence of a growth rate higher enough to compensate the loss rate a downward flux in the gyre core. Another common feature is low concentrations in the front part of the jet which could sign upward advection of water in the 27 -27.5 isopycnal band.

Sites (Leg 2)

The second leg observations confirm the spatial structure observed on the transect. The three profiles obtained at each site provide a visual estimation of the time and space variation in the cells distribution at the same location relative to the front.

Although *Prochlorococcus* stays the most abundant primary producer, its variation in abundance in surface is lower than on the transect. Figure 7 gives, for each site, three profiles which show a similar pattern except in site 4. A 40 m upper layer with constant concentrations, suggesting some amount of mixing, a gradient declining progressively to nearly 100 m and deeper, when sampled, low concentrations constant with depth. The upper mixed layer (Fig.4 and Table 3) is 30 m in Mediterranean waters (sites 8 and 2), 10-20 m in the north side of the jet (site 7), deepens at sites 4 and 5 and is 80 – 110 m in the gyre border and centre (sites 6 and 3). The sites related to the jet show a more complex vertical profile. A 20 to 30 m homogeneous layer is observed above a constant gradient of declining concentrations. The three profiles appear more different between them than do in the other sites. Although it is expected a difference between the morning and evening profiles, a spatial heterogeneity in the abundances in these frontal and jet site are suggested. The downward component

of the jet current which drives, along the isopycnal surface properties to the depth might be the origin of this heterogeneity. The deep maximum found in these profiles (70, 90, 120m) might be clues of such an entrainment on the isopycnal surfaces. The variability shown by these profiles should be the result of sampling in the sub-mesoscale structures associated with fronts and eddies (e.g. Klein & Lapeyre, 2009)

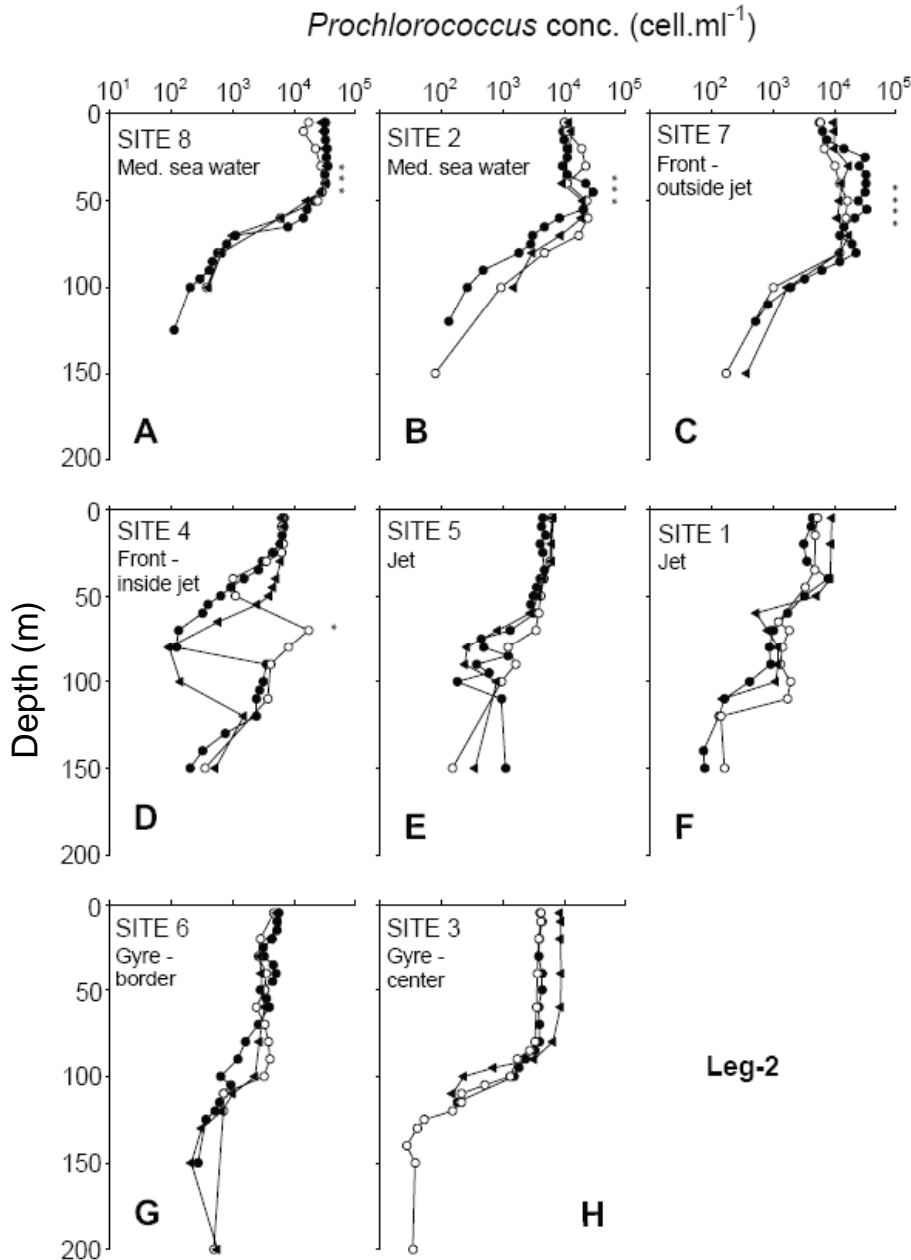


Figure 7: Vertical profiles of *Prochlorococcus* at the different sites investigated during leg-2. The three selected CTD were sampled at 8:00 (○) and 20:00 (●) of day 1 and at 8:00 (◄) of day 2 (local time). Small stars symbolize depths where two populations of *Prochlorococcus* were observed.

Profiles from sites 2 and 7 suggest a maximum of concentrations centred to 30 m and 40 m respectively, but clearly the deep maxima at site 7 is below the mixed layer depth there. The flow cytometer allowed us to observe there two distinct populations of *Prochlorococcus* with different chlorophyll fluorescence (e.g. Moore et al., 1998) at the bottom of homogeneous layer in Mediterranean waters (sites 8 and 3) and at the north side of the front (site 7), as well as in one sample in site 4.

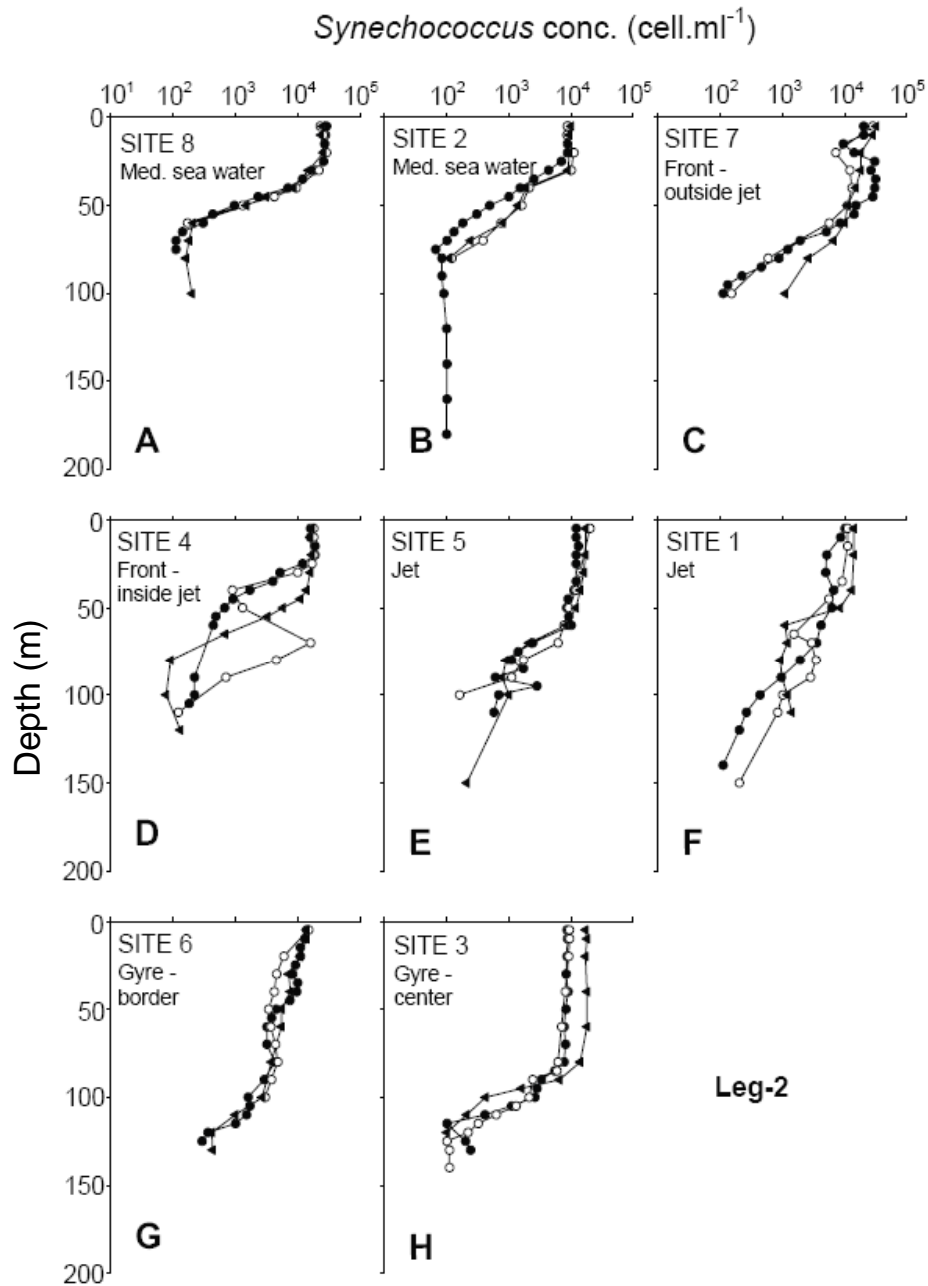


Figure 8 : Vertical profiles of *Synechococcus* at the different sites investigated during leg-2. The three selected CTD were sampled at 8:00 (○) and 20:00 (●) of day 1 and at 8:00 (◄) of day 2 (local time).

Synechococcus vertical profiles show nearly the same pattern as those from *Prochlorococcus* (Fig 8). However a closer examination shows some differences. In Mediterranean waters (site 8, 2), the homogeneous surface layer is shallower and the gradient steeper. The deep layer with constant concentration appears to start at 70 m. In the gyre waters (site 3) the gradient is the same as for *Prochlorococcus*. In the gyre border (site 6) the concentrations are declining slowly from surface to depth, as a remnant of the jet profile (site 1) which shows a constant declining gradient from surface to 150 m. The same type of variability in the profiles in the same site is found in the front inside the jet (site 4), strengthening the hypothesis on a physical entrainment of surface populations to depth.

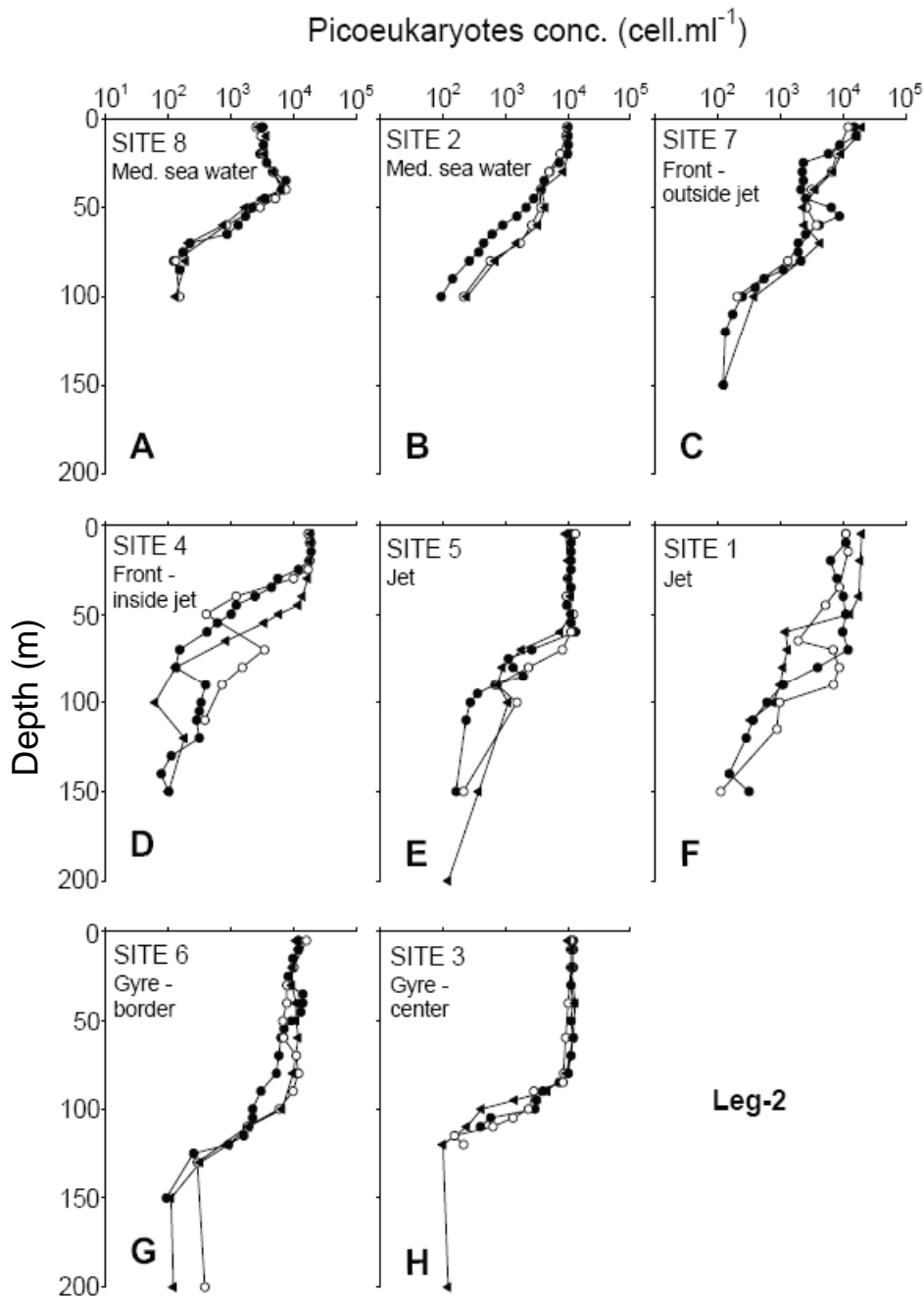


Figure 9: Vertical profiles of picoeukaryotes at the different sites investigated during leg-2. The three selected CTD were sampled at 8:00 (○) and 20:00 (●) of day 1 and at 8:00 (◄) of day 2 (local time).

The same remarks can be done about vertical profiles of picoeukaryotes concentrations (Fig 9). The general patterns are similar to the ones of the cyanobacteria. However in Med. waters there is a sub surface maximum in concentration (40 m), a shallow homogeneous layer in sites 2, 7 and 4, and a clear mixed surface layer down to 60 m in the jet (site 5). It should be noted that at site 3, in the gyre, the constant concentration layer of picoeukaryotes is deeper than observed in Leg 1. As for the other primary producers a large variation between successive profiles under the jet influence is observed at site 4 and also at site 1.

The primary producers profiles follow the density profile at most sites. The homogeneous layer depth is nearly the same as the mixed layer depth. At site 6 (gyre border) the profiles suggest a homogenous layer in *Prochlorococcus* and picoeukaryotes abundances when the density profile shows a gradient (Fig. 4). *Synechococcus* profile at the same site suggest also a gradient of abundance instead of an homogeneous concentration

Heterotrophic bacteria and VLPs which have been counted in surface layer (0-200 m) and in the deep layer (500-2000 m) show the same pattern of decrease with depth (Fig. 10). Heterotrophic bacteria at surface show a nearly constant concentration ($1 \cdot 10^6$ cells.ml⁻¹) except in the Mediterranean site 8 ($0.8 \cdot 10^6$ cells.ml⁻¹) and in the gyre site 3 ($0.09 \cdot 10^6$ cells.ml⁻¹). The concentrations in deep water (2000 m) are approximately two orders of magnitude less than in surface layer. The general pattern of the vertical profile for the two groups is a constant exponential decrease in abundance in surface layer which continues to 1000 m and below a constant concentration. It could be noted that the Levantine Intermediate water (LIW) observed at 400-500 m depths exhibit higher concentrations than the deep water of the western Mediterranean Sea. However no LIW, i.e. no deep salinity and temperature maxima was observed below the eastern gyre (eddy) (data not shown).

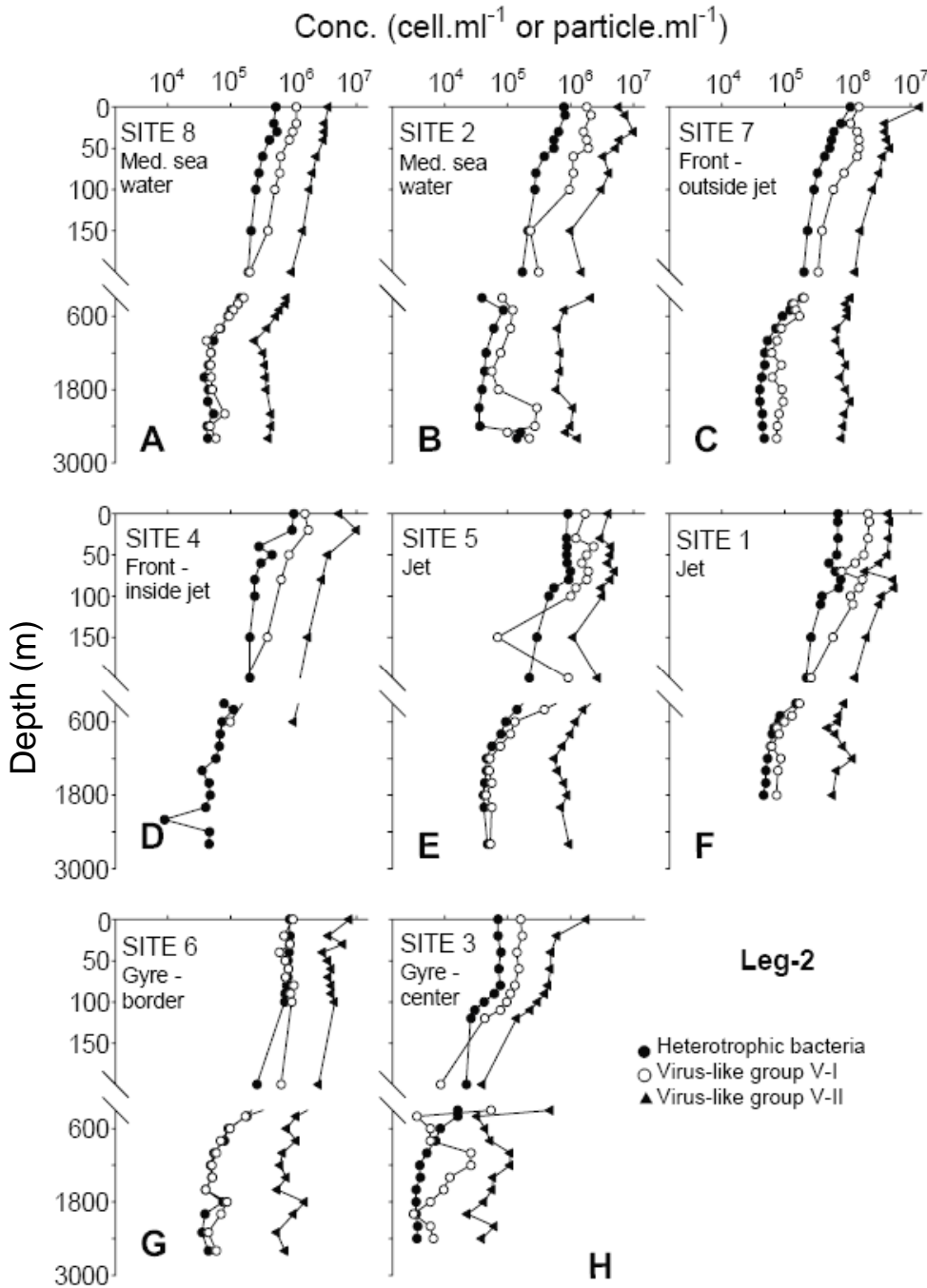


Figure 10:: Vertical profiles of heterotrophic bacteria and viruses over the entire water column at the different sites investigated during leg-2. This station was sampled at early night (between 20:00 and 22:00 local time).

The two groups of virus-like particles appear to decline with depth in the same way although the concentration of group V-I is nearly one order of magnitude smaller than group V-II. In the deep layer the abundance of V-I is much lower than V-II (1.5 orders of magnitude less), except in the gyre center (site 3). Some clear maxima can be observed in the deep layer at sites 2 and 3. This suggests some biological heterogeneity in the body of Mediterranean deep water in Alboran Sea. The ratio of total viruses to bacteria (VBR) was varying between 2 and 55 (12 on average). In surface waters (0-200 m) at site 6, viruses V-I and bacteria show the same abundance, whereas at other sites, viruses V-I were always more abundant than the bacterial community. At nearly all sites this difference was attenuated with depth (see sites 8, 7, 5, 1 and 6).

Carbon biomass distribution

Photosynthetic picoeukaryotes and bacteria contributed mostly to total carbon biomass (Fig. 11). There is a strong contrast between Mediterranean waters where bacteria biomass is larger than picoeukaryotes biomass, and the jet and gyre waters where the picoeukaryote biomass dominates. Carbon biomass of bacteria remained relatively constant in MED waters at $\sim 100 \mu\text{gC}\cdot\text{cm}^{-2}$, increased regularly to the South crossing the front, and is nearly constant in the jet and gyre waters at $\sim 200 \mu\text{gC}\cdot\text{cm}^{-2}$. However the increase in bacterial biomass from Med waters to gyre waters (nearly two fold) is clearly lower than that recorded for photosynthetic picoeukaryotes (5 to 6 fold increase, from 70 to $320 \mu\text{gC}\cdot\text{cm}^{-2}$).

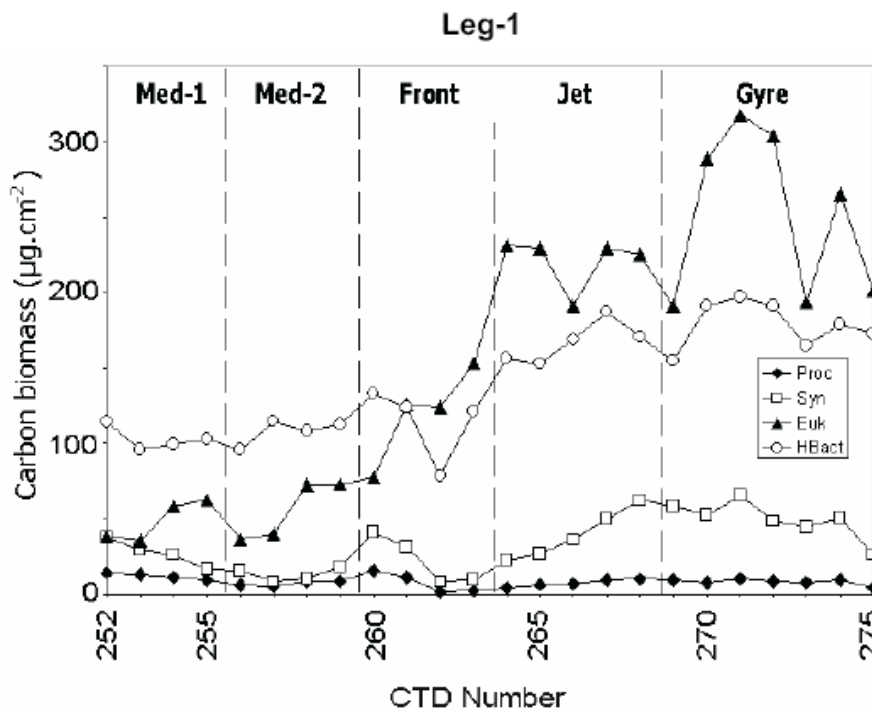


Figure 11: Carbon biomass concentration ($\mu\text{gC}\cdot\text{cm}^{-2}$) of *Prochlorococcus*, *Synechococcus*, picoeukaryotes and heterotrophic bacteria integrated over 0-100 m at each station of the transect 2 of leg-1.

Highest values recorded for carbon biomass were associated to the community of photosynthetic picoeukaryotes that dominated the C pool that increased significantly from Mediterranean waters towards the gyre (from 70 to $320 \mu\text{gC}\cdot\text{cm}^{-2}$). It is noteworthy that in MED-1 waters near the Spanish coast, the contribution of photosynthetic picoeukaryotes equalled that of *Synechococcus* at about $38 \mu\text{gC}\cdot\text{cm}^{-2}$. (Fig. 11). Highest C values for *Synechococcus* ($65 \mu\text{gC}\cdot\text{cm}^{-2}$) were recorded inside the gyre. *Prochlorococcus* carbon contribution was 2 to 3 fold higher at MED and frontal sites than in modified ATL waters (gyre waters) but that never exceeded 7% of the total (CTD 252 and 260, max $15 \mu\text{gC}\cdot\text{cm}^{-2}$).

Summing contributions of all picoplankton groups in the 0-100 m layer the highest total carbon biomass was recorded on Leg 1 in the southern part of the transect. Total carbon biomass of picoplankton was highest, first in the gyre (up to 590 $\mu\text{gC}\cdot\text{cm}^{-2}$ at CTD 271) and second in the jet (up to 475 $\mu\text{gC}\cdot\text{cm}^{-2}$ at CTD 267). By comparison, total carbon biomass was clearly less in the front (~ 290 $\mu\text{gC}\cdot\text{cm}^{-2}$ at CTD 261) and in MED waters (<220 $\mu\text{gC}\cdot\text{cm}^{-2}$).

A decrease in the total carbon biomass was measured between leg-1 and leg-2, especially in the gyre (up to 30%). However photosynthetic picoeukaryotes and bacteria still contributed mostly to total carbon biomass of picoplankton and the total contribution of other groups (i.e. *Prochlorococcus* + *Synechococcus* + viruses) never exceeded 20% (Fig. 12). There was a weak decrease of the contribution of bacteria to total picoplanktonic carbon biomass (from 50 to 40%) from Mediterranean sites to gyre sites.

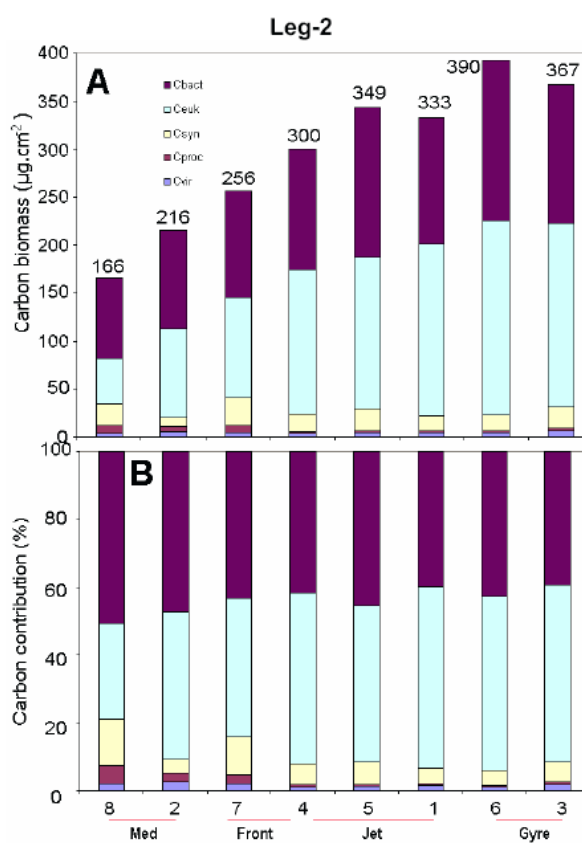


Figure 12 : Absolute (A) and relative (B) averaged carbon biomass integrated over 0-100 m for each site of the leg-2, given in $\mu\text{gC}\cdot\text{cm}^{-2}$ and % respectively of the whole microbial compartment composed of *Prochlorococcus*, *Synechococcus*, picoeukaryotes, heterotrophic bacteria and viruses.

As for leg 1, during leg-2, photosynthetic picoeukaryotes biomass increased significantly from north to south, from Mediterranean waters, site 8, to gyre waters, site 3 (from 45 to 200 $\mu\text{gC}\cdot\text{cm}^{-2}$). *Synechococcus* contribution to the C pool never exceeded 12% and the highest contribution was recorded at sites 8 and 7 (with 25-30 $\mu\text{gC}\cdot\text{cm}^{-2}$).

In ATL waters, from jet to gyre sites, *Synechococcus* contribution was very similar for the different sites and remained $<10\%$.

Although very small, *Prochlorococcus* carbon contribution was 2 to 3 fold higher at MED and frontal sites than in jet and gyre site. The contribution of viruses to carbon was very small and varied between 4.5 (site 4) and 10.5 $\mu\text{gC}\cdot\text{cm}^{-2}$ (site 3).

The proportion of particulate carbon (Cp) in the picoplankton fraction (<2 μm) compared to the <200 μm size fraction is summarized in table 4. The picoplankton contribution varied between 11% at site 4 and 53% at site 8.

Table 4: Contribution (in %) of picoplankton (fraction $< 2 \mu\text{m}$) to the total ($>0.2 \mu\text{m}$):

Chlorophyll *a* (Chl *a*); particulate carbon (Cp); particulate nitrogen (Np) at the depth of maximum of Chl *a* and 50% of surface light.

The corresponding concentrations at the depth of sampling for *Prochlorococcus* (*Proc.*), *Synechococcus* (*Syn.*), picoeucaryotes (Euk) and heterotrophic bacteria (H bact.) are given (numbers in $10^3 \text{ cell.ml}^{-1}$). Chl $<2 \mu\text{m}$, Cp $<2 \mu\text{m}$, and Np $<2 \mu\text{m}$ were not measured at site 1.

Site	CTD	Depth	Chl <i>a</i> < 2 μm	Cp < 2 μm	Np < 2 μm	<i>Proc.</i> -----	<i>Syn.</i> -x 10^3	Euk. cell.ml ⁻¹	Hbact. -----
2		50% light	22	35	27	11	10	10	810
2		max chl <i>a</i>	18	28	22	32	0.77	2.6	440
8	580	50% light	22	53	55	43	13	9.5	710
8	580	max chl <i>a</i>	24	27	32	41	31	3.5	600
7	536	50% light	26	31	26	35	36	4.4	520
7	536	max chl <i>a</i>	24	29	23	34	19	9.0	540
4	495	50% light	18	22	23	5.5	15	18	130
4	495	max chl <i>a</i>	4	11	20	0.98	0.71	1.4	630
5	508	50% light	16	34	28	4.2	13	13	1000
5	508	max chl <i>a</i>	16	19	20	4.2	12	13	1000
6	522	50% light	20	30	30	2.4	7.3	7.5	910
6	522	max chl <i>a</i>	12	33	20	5.9	1.5	13	830
3	428	50% light	18	20	23	4.9	11	11	1000
3	428	max chl <i>a</i>	49	19	46	4.0	9.2	11	980

Discussion

During the first part (leg-1) of the Almofront-2 cruise (winter 1997), the Almeria-Oran frontal – gyre structure was well marked with the Atlantic jet passing north of the anticyclonic gyre. This situation was different from the one recorded during the Almofront-1 cruise (spring 1991) where a second anticyclonic gyre was observed north of the Atlantic jet close to the Spanish coast. However the position of the jet north to the eastern anticyclonic gyre can fluctuate strongly in latitude (see figure 1 in Prieur & Sournia, 1994).

Clearly, no anticyclonic gyre was observed north to the jet during Almofront-2, but the southern one was fully developed and the frontal zone was observed as also found by Viudez *et al.* (1998) in 1992 and by Allen *et al.* (2001) in 1996. During the second leg, the anticyclonic gyre system moved slowly eastwards. In order to choose the sites for 36 h observations of leg-2, quick surveys were performed using an ADCP and a thermosalinograph. Then the ship was positioned in different part of the moving jet-eddy structure.

Correspondence between leg-2 sites and hydrodynamical structures recorded on the north-south transect (leg-1), is given by Cussat-Legras *et al.* (2001) and Prieur *et al.* (2003) and shown on figure 5.

Three physical zones could be discriminated and three types of systems, based on picoplankton distribution, could be defined: the Mediterranean system in the Northern part, the Atlantic water anticyclonic gyre system in the southern part, and the frontal system in-between. In the following paragraphs, we discuss each situation and document how frontal mesoscale features strongly influence the environment which controls picoplankton distribution (i.e. nutrient, light, and mixing).

Mediterranean ecosystem

Typical MED waters were relatively oligotrophic with concentrations of nitrates and phosphates in surface layer lower than 0.06 and 0.02 $\mu\text{mol.l}^{-1}$, respectively (Table 1), resulting in the lowest carbon biomass registered in the Alboran Sea during the cruise (Fig. 12). Not surprisingly, *Prochlorococcus* was found to be the most abundant picophytoplankton group (e.g. Partensky *et al.*, 1999), especially at depth larger than 30 m (site 2) and in typical MED waters. This result is in agreement with the observations of Moran *et al.* (2001) in typical MED waters surrounding the Algerian current, further East, on October 1996, who showed the dominance of *Prochlorococcus* over the other picophytoplankters in the 0-90 m layer.

It is noteworthy that, at site 2, the differences of concentrations between *Prochlorococcus*, *Synechococcus* and picoeukaryotes in the 0-30 m surface layer were very small and *Prochlorococcus* only dominated over the two other groups from 30 m to nearly 100 m, the bottom of the euphotic layer. This suggests that this site was not highly oligotrophic and that the frontal hydrodynamical structure (as inferred from gradients of temperature, salinity and current speed) and internal waves induced an horizontal spreading or injection of nutrient in the nearby Mediterranean surface waters (Fasham *et al.*, 1985). A similar fertilization had already been reported during Almofront-1 (Videau *et al.*, 1994). Site 8 was clearly more oligotrophic with picoeukaryotes one order of magnitude less concentrated than *Synechococcus* in surface waters. In a parallel study, Van Wambeke *et al.* (2004) also showed clear differences between sites 2 and 8 with primary production 3 time higher and bacterial production 1.5 times higher at site 2 than at site 8. The two groups of *Prochlorococcus* with different chlorophyll fluorescence signatures regularly observed at depths about 30 to 50 m in MED waters, correspond probably to genetically distinct ecotypes (Moore & Chisholm, 1999; Ahlgren *et al.*, 2006; Zwirgmaier *et al.*, 2008) The absence of variations in water density profiles at MED stations (site 2 and 8) suggests that these populations do not originate from different water masses, in agreement with previous records for the NW Mediterranean Sea (Vaulot & Partensky, 1992).

Such a high correlation between *Prochlorococcus* and *Synechococcus* concentration was previously reported in Mediterranean waters in winter, suggesting that the two populations may respond very similarly to changes in their environment including nutrient, light and temperature (Vaulot *et al.*, 1990; Zwirgmaier *et al.*, 2008). HPLC analysis also revealed that zeaxanthin (mostly characteristic of cyanobacteria, Claustre, 1994) was a major pigment in these waters. Thus, it is not surprising that the contribution of picoplankton to the total <200 μm fraction reached nearly 55% in terms of carbon and 24% in terms of Chl *a* in agreement with Morán *et al.* (2001). The lack of large cells as inferred from results obtained with an automatic counter of particles (Sciandra, person. com.), low abundance of zooplankton (Youssara & Gaudy, 2001) as well as important absorption and regeneration rates for ammonium (Madec *et al.*, person. com.) in addition to the previous features suggest that MED waters were characteristics of a relatively oligotrophic ecosystem, possibly influenced by nutrient-richer adjacent or deeper waters. At last, local enrichment could also be inferred from the presence during leg-1 of a clear maximum of Chl *a* at 30-40 m in MED-2 waters.

Frontal ecosystem

The Alboran frontal system is a near permanent structure created by the jet current entering the Mediterranean sea. The eastern part of the front is located between Almeria (Spain) and Oran (Algeria) but its geographical extension to the north varies. During the Almofront 2 cruise it is detected to the south of the Almeria-Oran area. The strong gradients, which are its major characteristic, occurs as a 10 to 30 km wide meandering strip in the 100 to 200 m deep upper layer. It is a typical mesoscale structure. A consequence of the secondary circulation is an upward advection of water rich in nutrients and as expected a primary production in this region essentially based on diatoms (Claustre *et al.*, 2000) This biological enhancement was clearly observed in the left side of the frontal system, where water is upwelled and not on the right side, near the gyre, where water is downwelled (see figures 3 and 6). Such high diatom production had already been recorded in May 1991 during Almofront-1 (Claustre *et al.*, 1994, Videau *et al.*, 1994) suggesting that it is a permanent frontal feature in the Alboran Sea.

High concentrations of both *Prochlorococcus* and *Synechococcus* were also observed in the left side of the front although high concentrations of both populations recorded at this place could thus be due to MED populations exported downward in the secondary circulation, along the isopycnals and benefiting of the mixing with upward transport of nutrient rich water, as suggested by Zakardjian & Prieur (1998) in the Ligurian Sea frontal system's and modeled by Zakardjian (1994) in the Alboran Sea. Consequently, the contribution of picoplankton to Chl *a* was significant at site 7, reaching 25%. Cyanobacterial enhancement could also be explained by other factors such as sufficient light reaching the cells or the impossibility for potential grazers to adapt rapidly (Jacquet *et al.*, 2002). Van Wambeke *et al.* (2004) observed indeed clear differences among sites in terms of grazing efficiency by heterotrophic nanoflagellates, with very low values in the front. The potential role of light control could be inferred from the distribution of picoeukaryotes. Indeed, the absence of any peak of eukaryotes, in contrast to cyanobacteria, both recorded during leg-1 and 2 suggested indeed that this group was controlled differently than cyanobacteria. As nutrients were likely not to be limiting (see table 1), inefficient grazing and water stability were more likely factors affecting cyanobacteria such as *Prochlorococcus* (Partensky *et al.*, 1999).

It is possible that the MED picoeukaryotic populations could only sustain rapid growth at higher level of light (Jacquet *et al.*, 2002). In the central part of the front, the low concentration of *Prochlorococcus* was probably related to the lack of column stability that seems to be a prerequisite for *Prochlorococcus* growth and development (Lindell & Post, 1995; Bustillos-Guzman *et al.*, 1995). In contrast, maximum *Synechococcus* abundances were recorded within these semi-mixed water conditions where nitrates were in excess. Such high *Synechococcus/Prochlorococcus* ratio in nitrates rich waters has been often reported (Tarran *et al.*, 1999; Partensky *et al.*, 1999; Furnas & Crosbie, 1999).

Heterotrophic bacteria concentration clearly increased from MED-1 to the jet waters from Leg 1 transect. The high concentration of heterotrophic bacteria recorded at 40-50 m in the north side of the front was clearly associated to the maximal concentration of Chl *a* as observed also in MED-2 waters. As heterotrophic bacterial and primary productions were well correlated (Van Wambeke *et al.*, 2004), it is possible that the former was dependent on the later (see above). Alternatively, bacteria could also take advantage of the high level of nutrients advected by the secondary circulation since they were nutrient limited in MED waters. Interestingly, during Almofront-1, phytoplankton production was not used by local bacteria in surface waters of the front in spring (Fernandez *et al.*, 1994). During Almofront-2, heterotrophic bacteria concentration, inside the front, remained relatively low, contrasting with high bacterial production (Van Wambeke *et al.*, 2004). Such a de-coupling between biomass and production could be due to an efficient top down control, i.e. grazing pressure by protozoans but this apparently was not the case (Van Wambeke *et al.*, 2004). Hence, the likely explanation is that both strong vertical (up to 5 m.day⁻¹) water mass motions could transfer the produced bacterial biomass towards the right side of the jet, i.e. toward the gyre water, before grazing pressure could efficiently proceed. Such a hypothesis holds when considering the large amount of heterotrophic bacteria recorded in the south side of the front. Such an increase of bacterial abundance and carbon biomass through the front has also been recorder in leg-2 observations (Fig. 11).

Modified atlantic waters and gyre ecosystems

From the transect as well as from sites profiles it is clear that inside the gyre, the carbon biomass of picoplankton was the highest compared to MED and frontal waters. At this place (site 6), the highest value for phytoplankton depth integrated biomass was also recorded (Tolosa *et al.*, 2004; Leblanc *et al.*, 2004). The contribution of picoplankton to total carbon and Chl *a* was as high as 33% and 49%, respectively (see Table 4). It was essentially due to picoeukaryotes, especially in the centre of the gyre. HPLC measurements revealed that there was an important concentration of the carotenoids 19'HF and 19'BF, revealing the potential predominance of prymnesiophytes and pelagophytes (Claustre, 1994; Vaultot *et al.*, 2008). Correlations between picoeukaryote abundance and 19'HF pigment suggesting a fixed contribution of Prymnesiophytes to picoeukaryotes were previously observed in the Alboran Sea

by Barlow *et al.* (1995, 1997) and during Almofront-1 (Fiala *et al.*, 1994). In fact, prymnesiophytes seem to be a major and relatively diverse eukaryotic component in many oceanic provinces (Wilmotte *et al.*, 2002; Fuller *et al.*, 2006; Mc Donald *et al.*, 2007).

Bacterial biomass was the highest of the 3 ecosystems although bacterial production was only half that recorded in the frontal zone (Van Wambeke *et al.*, 2004). Such a situation was already recorded during Almofront-1 (Fernandez *et al.*, 1994) and was likely due to different grazing efficiencies and biomass exportation (Van Wambeke *et al.*, 2004). Interestingly, we found that nitrites were clearly higher in these modified ATL waters than in the two previous ecosystems (Table 1). Such a relationship between heterotrophs and nitrites strongly suggest that these waters were characterized by high rates of regeneration processes. Bianchi *et al.* (1994) reported the same observation during Almofront-1 in spring suggesting that the gyre may keep these characteristics in time and space. Van Wambeke *et al.* (2004) showed that bacteria were not limited by any food resource in these modified Atlantic waters. Thus the gyre ecosystem appeared as a mesotrophic system in which bacterial production was likely sustained by lateral incomes from the frontal area. The distribution of *Synechococcus*, also well represented in surface layers of the gyre, corresponds to that usually found in a mesotrophic ecosystem (e.g. Partensky *et al.*, 1996, 1999). In view of the elevated concentration of picoplankton in the gyre and of the gradient of concentration recorded between the three ecosystems, it is likely that its production was important in these waters. These observations show that the gyre ecosystem appeared as a mesotrophic system.

Distribution and potential role of viruses

Virus concentrations fell in the range previously reported for Mediterranean waters by Marie *et al.* (1999) from FCM measurements, but considerably higher than those of Alonso *et al.* (2001) who used both epifluorescence and electron transmission microscopy. They reported concentrations varying between 3×10^3 and 8×10^4 virus ml^{-1} in summer in the Alboran Sea which are much lower than those reported in the literature and we suspect them to be biased. Our measurements of the total viral concentration (3×10^5 to 2×10^7 virus ml^{-1}) and of viruses to bacteria ratios (VBR, between 2 and 55) are in agreement with typical values now accepted (see reviews by Maranger & Bird, 1995; Fuhrman, 1999; Wommak & Colwell, 2000; Weinbauer *et al.*, 2003; Suttle, 2005, 2007). The higher number of viral particles in surface waters and their exponential decrease with depth, following that of bacteria and other organisms in the 0-200m layer, indicated that viruses were closely related to biological activity (Hara *et al.*, 1996). The existence of the two populations referred to as V-I and V-II is in agreement with a previous profile obtained for the Mediterranean Sea by Marie *et al.* (1999). According to FCM scatter and fluorescence, V-I particles were larger than V-II, suggesting that the V-I could be infectious to eukaryotic phytoplankton while V-II could be bacteriophages (Jacquet *et al.*, 2002; Marie *et al.*, 1999).

However, clear significant statistical correlations were only found between viruses and heterotrophic bacteria (N total virus versus N bacteria : $r=0.72$, $p=0.05$, $n=385$) as often reported (Boehme *et al.*, 1993; Cochlan *et al.*, 1993; Alonso *et al.*, 2001; Middelboe, 2008). This suggests that heterotrophic bacteria were the main hosts of the viruses. The lack of significant correlations between virus V-I as well as V-II and bacterial abundances, when considering the whole water column, is not surprising because in the Ligurian sea, Winter *et al.* (2009) have shown that viruses are related to prokaryotes in very different ways in epi-, meso- and bathypelagial domains. High VBR could suggest high infection rates, high number of viral particles for each bacterial host and/or low virus decay rates.

Vertical profiles of bacterial abundance in the Alboran Sea are similar in shape to those obtained in the Ligurian Sea by Tanaka *et al.* (2005). The deep maximum in viral abundance observed at some sites (site 3 at 1000 m; site 2 at 2000 m) has also been observed in the Ligurian Sea (Weinbauer *et al.*, 2003)

Conclusion

The Alboran Sea constitutes a perfect area to investigate the coupling between biological and physical processes mainly because the major structures (front and anticyclonic eddies) are more or less stationary in space. The transect across Alboran sea (leg-1) and the sites sampling (leg-2) have shown that spatial structure can be represented by 3 typical elements

(1) Med ecosystem influenced by Mediterranean water from the north of Balearic-Algerian basin:

(2) Gyre ecosystem accumulating Atlantic water progressively modified by mixing with Mediterranean waters,

(3) Frontal ecosystem at the boundary of the two previous systems, characterized by strong horizontal gradients in the physical and biological parameters.

The secondary circulation associated with the jet current gives this system dynamical properties through upwelling and downwellings along isopycnals. Nutrient enrichment as well as dynamic stationarity provided by the upward transport is favourable to autotrophic growth.

Fronts are relatively frequent in the ocean and their influence may be significant at regional and global scales. Our data on picoplankton contribute to the quantification of role of fronts in upper layer of the sea. To date, only a few data on the distribution of microbial communities are available for the open Mediterranean Sea (Magazzu & Decembrini, 1995; Martín-Cuadrado *et al.*, 2007) by comparison to coastal waters (Ghiglione *et al.*, 2005; Sala *et al.*, 2006; Alonso-Sáez *et al.*, 2007).

Almofront-2 cruise allowed us to obtain an unprecedented synoptic view of the distribution and standing stocks of picoplanktonic groups and viruses, analyzed by flow cytometry, which revealed a high variability. During winter season, relatively oligotrophic areas were dominated by *Prochlorococcus* whereas *Synechococcus* and picoeukaryotes were more common in the upper layer well illuminated and nutrient rich of the “modified Atlantic waters” related to the eastern Alboran gyre.

Alboran Sea has been a good model to test the paradigm of phytoplankton. This paradigm states that picoplankton constitute a constant background community limited by diffusive processes, water stability and top down control while opportunistic species (larger cells) respond rapidly to nutrient enrichment with a clear de-coupling of control by higher trophic levels (Fiala *et al.*, 1994). If the data obtained during Almofront-2 cruise do not change this general scheme, it is noteworthy however that picoplankton represents a sizeable part of the total living carbon biomass and seems to display very variable response to the hydrodynamically active frontal structures. This should be considered in the development of predictive models dealing with the coupling between physical and biological variables, especially for quantifying carbon fluxes.

References

- AHLGREN, N. A., ROCAP, G. & CHISHOLM, S. W., 2006. Measurement of *Prochlorococcus* ecotypes using real-time polymerase chain reaction reveals different abundances of genotypes with similar light physiologies. *Environmental Microbiology*, 8:441-454.
- ALLEN, J. T., SMEED, D. A., TINTORÉ, J. & RUIZ, S., 2001. Mesoscale subduction at the Almeria Oran front Part1: A geostrophic flow. *Journal of Marine Systems*, 30:263-285.
- ALONSO, M. C., JIMENEZ-GOMEZ, F., RODRIGUEZ J. & BORREGO, J. J., 2001. Distribution of virus-like particles in an oligotrophic marine environment (Alboran Sea, Western Mediterranean). *Microbial Ecology*, 42:407-415.
- ALONSO-SÁEZ, L., BALAGUÉ, V., SÀ, E. L., SÁNCHEZ, O., GONZÁLEZ, J. M., PINHASS, J., MASSANA, R., PERNTHALER, J., PEDRÓS-ALIÓ, C., & GASOL, J. M., 2007. Seasonality in bacterial diversity in north-west mediterranean coastal waters: assessment through clone libraries, fingerprinting and FISH. *FEMS Microbiology Ecology*, 60:98-112.
- AZAM, F., FENCHEL, T., FIELD, J.G., GRAY, J. S., MEYER-REIL, L. A. & THINGSTAD, F.,

1983. The ecological role of water-column microbes in the sea. *Marine Ecology Progress Series*, 10:257-263.
- BARLOW, R. G., MANTOURA, R. F. C., CUMMINGS, D. G. & FILEMAN, T. W., 1997. Pigment chemotaxonomic distributions of phytoplankton during summer in the Western Mediterranean. *Deep-Sea Research I*, 44:833-850.
- BERGH, O., BORSHEIM, K. Y., BRATBAK, G. & HELDAL, M., 1989. High abundances of viruses found in aquatic environments. *Nature*, 340:467-468.
- BIANCHI, M., MORIN, P. & LE CORRE, P., 1994. Nitrification rates, nitrite and nitrate distribution in the Almeria-Oran frontal systems (eastern Alboran Sea). *Journal of Marine Systems*, 5:327-342.
- BOEHME, J., FRISCHER, M. E., JIANG, S. C., KELLOGG, C. A., PICHARD, S., ROSE, J. B., STEINWAY C. & PAUL, J. H., 1993. Viruses, bacterioplankton, and phytoplankton in the southeastern Gulf of Mexico: distribution and contribution to oceanic DNA pools. *Marine Ecology Progress Series*, 97:1-10.
- BOWER, A. S. & ROSSBY, T., 1989. Evidence of cross frontal exchange processes in the Gulf Stream based on isopycnals float data. *Journal of Physical Oceanography*, 19:1177-1190.
- BRATBAK, G., HELDAL, M., THINGSTAD, T. F., RIEMANN, B. & HASLUND, O. H., 1992. Incorporation of viruses into the budget of microbial C-transfer: A first approach. *Marine Ecology Progress Series*, 83:273-280.
- BUSTILLOS-GUZMAN, J., CLAUSTRE, H. & MARTY, J. C., 1995. Specific phytoplankton signatures and their relationship to hydrographic conditions in the coastal northwestern Mediterranean sea. *Marine Ecology Progress Series*, 124:247-258.
- CAMPBELL, L., NOLLA, H. A. & VAULOT, D., 1994. The importance of *Prochlorococcus* to community structure in the central North Pacific Ocean. *Limnology and Oceanography*, 39:954-961.
- CHENEY, R. E. & DOBLAR, R. A., 1982. Structure and variability of the Alboran Sea frontal system. *Journal of Geophysical Research*, 87:585-594.
- CLAUSTRE, H., 1994. Phytoplankton pigment signatures of the trophic status in various oceanic regimes. *Limnology and Oceanography*, 39:1207-1211.
- CLAUSTRE, H., KEHERVÉ, P., MARTY, J.-C., PRIEUR, L., VIDEAU C. & HECQ, J.-H., 1994. Phytoplankton dynamics associated with a geostrophic front: ecological and biogeochemical implications. *Journal of Marine Research*, 52:711-742.
- CLAUSTRE, H., FELL, F., OUBELKHEIR, K., PRIEUR, L., SCIANDRA, A., GENTILI, B. & BABIN, M., 2000. Continuous monitoring of surface optical properties across a geostrophic front: biogeochemical inferences. *Limnology and Oceanography*, 45:309-320
- COCHLAN, W. P., WIKNER, J., STEWARD, G. F., SMITH D. C. & AZAM, F., 1993. Spatial distribution of viruses, bacteria and chlorophyll *a* in neritic, oceanic and estuarine environments. *Marine Ecology Progress Series*, 92:77-87.
- CUSSATLEGRAS A.S., GEISTDOERFER, P. & PRIEUR, L., 2001. Planktonic bioluminescence measurements in the frontal zone of Almeria - Oran (Mediterranean Sea). *Oceanologica Acta*, 24:239-250.
- CUTTELOD, A. & CLAUSTRE, H., 2010. ALMOFRONT 2 cruise in Alboran sea: Chlorophyll fluorescence calibration. *Journal of Oceanography, Research and Data*, 3 (2) : 6-11.
- DÍEZ, B., PEDRÓS-ALIÓ, C. & MASSANA, R., 2001. Study of genetic diversity of eukaryotic picoplankton in different oceanic regions by small-subunit rRNA gene cloning and sequencing. *Applied and Environmental Microbiology*, 67:2932-2941.
- DUCKLOW, H. W., 1999. The bacterial component of the oceanic euphotic zone. *FEMS Microbiology Ecology*, 30: 1-10.
- FARMER, D. M. & ARMI, L., 1988. The flow of Atlantic water through the strait of Gibraltar. *Progress in Oceanography*, 21:1-41.
- FASHAM, M. J. R., PLATT, T., IRWIN, B. & JONES, K., 1985. Factors affecting the spatial pattern of the deep chlorophyll maximum in the region of the Azores front. *Progress in Oceanography*, 14:129-165.

- FERNANDEZ, M., BIANCHI, M. & Van WAMBEKE, F., 1994. Bacterial biomass, heterotrophic production and utilization of dissolved organic matter photosynthetically produced in the Almeria-Oran front. *Journal of Marine Systems*, 5:313-325.
- FIALA, M., SOURNIA, A., CLAUSTRE, H., MARTY, J.-C., PRIEUR, L. & VÉTION, G., 1994. Gradients of phytoplankton abundance, composition and photosynthetic pigments across the Almeria-Oran front (SW Mediterranean Sea). *Journal of Marine Systems*, 5:223-233.
- FRANKS, P. J. S., 1992. Sink or swim: accumulation of biomass at fronts. *Marine Ecology Progress Series*, 82:1-12.
- FULLER, N.J., TARRAN, G.A., CUMMINGS, D., WOODWARD, E.M.S., ORCUTT, K.M., YALLOP, M., LE GALL, F., & SCANLAN, D.J., 2006. Molecular analysis of photosynthetic picoeukaryote community structure along an Arabian Sea transect. *Limnology and Oceanography*, 51:2502-2514.
- FUHRMAN, J. A., 1999. Marine viruses and their biogeochemical and ecological effects. *Nature*, 399:541-548.
- FURNAS, N. D. & CROSBIE, N. D., 1999. *In situ* growth dynamics of the photosynthetic picoplankters *Synechococcus* and *Prochlorococcus*. Marine Cyanobacteria, Charpy, L. and Larkum, A. W. D. (Eds). *Bulletin de l'Institut Océanographique*, Monaco, n° special 19: 387-417.
- GHIGLIONE, J.F., LARCHER, M. & LEBARON, P., 2005. Spatial and temporal scales of variation in bacterioplankton community structure in NW Mediterranean Sea. *Aquatic Microbial Ecology*, 40:229-240.
- GOULD, R. W. Jr. & WIESENBERG, D. A., 1990. Single-species dominance in a subsurface phytoplankton concentration at a Mediterranean Sea front. *Limnology and Oceanography*, 35:211-220.
- HARA, S., KOIKE, I., TERAUCHI, K., KAMIYA H. & TANOUE, E., 1996. Abundance of viruses in deep oceanic waters. *Marine Ecology Progress Series*, 145:269-277.
- JACQUET, S., LENNON, J.-F., MARIE D. & VAULOT, D., 1998. Picoplankton population dynamics in coastal waters of the NW Mediterranean Sea. *Limnology and Oceanography*, 43:1916-1931.
- JACQUET S., HAVSKUM, H., THINGSTAD, F. T. & VAULOT, D., 2002. Effects of inorganic and organic nutrient addition on a coastal microbial community (Isefjord, Denmark). *Marine Ecology Progress Series*, 228:3-14.
- JACQUET, S., MIKI, T., NOBLE, R., PEDUZZI P. & WILHELM, S., 2010. Viruses in aquatic ecosystems: important advancements of the last 20 years and prospects for the future in microbial oceanography and limnology. *Advance in Oceanography and Limnology*, 1: 71-101.
- KLEIN, P. & LAPEYRE, G., 2009. The oceanic vertical pump induced by mesoscale and submesoscale turbulence. *Annual Review of marine Science*, 1: 351-375.
- LEBLANC, K., QUEGUINER, B., PRIEUR, L., CLAUSTRE, H. & OUBELKHEIR, K., 2004. Siliceous phytoplankton production and export related to trans-frontal dynamics of the Almeria-Oran frontal system (Western Mediterranean Sea) during winter. *Journal of Geophysical Research*, 109C07010, doi:10.1029/2003JC001878.
- LEE, S. & FUHRMAN, J. A., 1987. Relationships between biovolume and biomass of naturally derived marine bacterioplankton. *Applied and Environmental Microbiology*, 53:1298-1303.
- LI, W. K. W. 1994. Phytoplankton biomass and chlorophyll concentration across the North Atlantic. *Scientia Marina*, 58:67-79.
- LINDELL, D. & POST, A. F., 1995. Ultraphytoplankton succession is triggered by deep winter mixing in the Gulf of Aqaba (Eilat), Red Sea. *Limnology and Oceanography*, 40:1130-1141.
- MAGAZZÙ, G. & DECEMBRINI, F., 1995. Primary production, biomass and abundance of phototrophic picoplankton in the Mediterranean Sea: a review. *Aquatic Microbial Ecology*, 9:97-104.
- MARANGER, R. & BIRD, D. F., 1995. Viral abundance in aquatic systems: a comparison between marine and fresh waters. *Marine Ecology Progress Series*, 121:217-226.
- MARAÑÓN, E., HOLLIGAN, P. M., BARCIELA, R., GONZALEZ, N., MOURINO B., PAZO, M. J. & VARELA, M., 2001. Patterns of phytoplankton size structure and productivity in contrasting

- open-ocean environments, *Marine Ecology Progress Series*, 216:43–56.
- MARIE, D., PARTENSKY, F., JACQUET, S. & VAULOT, D., 1997. Enumeration and cell cycle analysis of natural populations of marine picoplankton by flow cytometry using the nucleic acid dye SYBR-Green I. *Applied and Environmental Microbiology*, 63:186-193.
- MARIE, D., BRUSSAARD, C., BRATBAK, G., & VAULOT, D., 1999. Enumeration of marine viruses in culture and natural samples by flow cytometry. *Applied and Environmental Microbiology*, 65:45-52.
- MARIE, D., ZHU, F., BALAGUE, V., RAS, J. & VAULOT, D., 2006. Eukaryotic picoplankton communities of the Mediterranean Sea in summer assessed by molecular approaches (DGGE, TTGE, QPCR). *FEMS Microbiology Ecology*, 55, 403-415.
- MARTÍN-CUADRADO, A. B., LÓPEZ-GARCÍA, P., ALBA, J. C., MOREIRA, D., MONTICELLI, L., STRITTMATTER A., GOTTSCHALK G. & RODRIGUEZ-VALERA, F., 2007. Metagenomics of the deep Mediterranean, a warm bathypelagic habitat. *PLoS ONE*, 2(9): e914. doi:10.1371.
- MIDDELBOE, M., 2008. Microbial disease in the sea: Effects of viruses on carbon and nutrient cycling. In Ostfeld, R.S., Keesing, F. and Eviner, V.T. (eds.): *Infectious disease ecology: Effects of ecosystems on disease and of disease on ecosystems*. Princeton University Press, Princeton, NJ: 242-259.
- MINAS, H.-J., COSTE, B., LE CORRE, P., MINAS, M. & RAIMBAULT, P., 1991. Biological and geochemical structures associated with the water circulation through the strait of Gibraltar and in the western Alboran Sea. *Journal of Geophysical Research*, 96:8755-8711.
- MOORE, L. R., ROCAPP, G. & CHISHOLM, S.W.. 1998. Physiology and molecular phylogeny of distinct ecotypes of *Prochlorococcus* coexisting in the oceanic euphotic zone. *Nature*, 393:464-467.
- MOORE, L. R. & CHISHOLM, S. W., 1999. Photophysiology of the marine cyanobacterium *Prochlorococcus*: Ecotypic differences among cultured isolates. *Limnology and Oceanography*, 44:628-638.
- MORAN, X. A. G., TAUPIER-LETAGE, I., VASQUEZ-DOMINGUEZ, E., RUIZ, S., ARIN, L., RAIMBAULT, P. & ESTRADA, M., 2001. Physical-biological coupling in the Algerian Basin (SW Mediterranean): Influence of mesoscale instabilities on the biomass and production of phytoplankton and bacterioplankton. *Deep-Sea Research I*, 48:405-437.
- PARTENSKY, F., BLANCHOT, J., LANTOINE, F., NEVEUX, J., & MARIE, D., 1996. Vertical structure of picoplankton at different trophic sites of the subtropical Atlantic Ocean. *Deep-Sea Research I*, 43:1191-1213.
- PARTENSKY, F., BLANCHOT, J. & VAULOT, D., 1999. Differential distribution and ecology of *Prochlorococcus* and *Synechococcus*: a review. In Marine Cyanobacteria, Charpy, L. and Larkum, A. W. D. (Eds). *Bulletin de l'Institut Océanographique*, Monaco, n° spécial 19 : 431-449.
- PRIEUR, L., COPIN-MONTEGUT C., & CLAUSTRE, H., 1993. Biophysical aspects of “Almofront-1”, an intensive study of a geostrophic frontal jet. *Annales de l'Institut Océanographique*, 69:71-86.
- PRIEUR, L. & SOURNIA, A., 1994. "Almofront-1" (April-May 1991): an interdisciplinary study of the Almeria-Oran geostrophic front, SW Mediterranean Sea. *Journal of Marine Systems*, 5:187-203.
- PRIEUR, L., LEFEVRE, D., GORSKY, G., Van WAMBEKE, F., BIANCHI, M., ANDERSEN V. & GRATTON, Y., 2003. Frontal processes enhance productivity of the Alboran Sea: a tentative first synthesis of the Almofront 2 experiment results. EGS-AGU-EGU Joint Assembly, Nice, 06-11 April 2003, presentation *presnice-2003.ppt* available on web site: http://www.obs-vlfr.fr/cd_rom_dmtt/fr_main.htm under results
or on ftp site:
ftp://oceane.obs-vlfr.fr/pub/prieur/almofront/almofront2/almofron2_pubrapp/EGUnice2003/

- RODRÍGUEZ, J., TINTORÉ, J., ALLEN, J.T., BLANCO, J.M., GOMIS D., REUL, A., RUIZ, J., RODRÍGUEZ, V., ECHEVARRÍA, F. & JIMÉNEZ-GÓMEZ, F., 2001. Mesoscale vertical motion and the size structure of phytoplankton in the ocean. *Nature*, 410:360-363.
- SALA, M., ESTRADA M. & GASOL, J. P., 2006. Seasonal changes in the functional diversity of bacterioplankton in contrasting coastal environments of the NW Mediterranean. *Aquatic Microbial Ecology*, 44:1-9.
- SEMPÉRÉ, R., DAFNER, E., Van WAMBEKE, F., LEFÈVRE, D., MAGEN, C., ALLÈGRE S., BRUYANT, F., BIANCHI, M. & PRIEUR, L., 2003. Distribution and cycling of total organic carbon across the Almeria-Oran Front in the Mediterranean Sea: Implications for carbon cycling in the western basin, *Journal of Geophysical Research*, 108(C11), 3361, doi:10.1029/2002JC001475,
- SUTTLE, C. A., 2005. Viruses in the sea. *Nature*, 437: 356-361.
- SUTTLE, C. A., 2007. Marine viruses - Major players in global ecosystem. *Nature Reviews Microbiology*, 5:801-812.
- TANAKA, T. & RASSOULZADEGAN, F., 2002. Full-depth profile (0-2000m) of bacteria, heterotrophic nanoflagellates and ciliates in the NW Mediterranean Sea. Vertical partitioning of microbial trophic structures. *Deep-Sea Research I*, 49: 2093-2107.
- TARRAN, G. A., BURKILL, P. H., EDWARDS E. S. & WOODWARD, E. M. S., 1999. Phytoplankton community structure in the Arabian Sea during and after the SW monsoon, 1994. *Deep-Sea Research I*, 46:655-676.
- THINGSTAD, T. F., BRATBAK, G., HELDAL, M. & DUNDAS, I., 1997. Trophic interactions controlling the diversity in pelagic microbial food webs. *Progress in Microbial Ecology*, Martins, M. T. et al (eds) Brazilian Society for Microbiology.
- TINTORÉ, J., LA VIOLETTE, P. E., BLADE I. & CRUZADO, A., 1988. A study of an intense density front in the eastern Alboran Sea: the Almeria-Oran front. *Journal of Physical Oceanography*, 18:1384-1397.
- TOLOSA, I., VESCOVALI, I., LEBLOND, N., MARTY, J.-C., DE MORA, S., & PRIEUR, L., 2004. Distribution of pigment and fatty acids biomarkers in particulate matter from the frontal structure of the Alboran Sea (SW Mediterranean Sea). *Marine Chemistry*, 88 : 103-125.
- TORSVIK, V., OVREAS L. & THINGSTAD, F.T., 2002. Prokaryotic diversity – magnitude, dynamics and controlling factors. *Science*, 296:1064-1066.
- TREGUER, P. & Le CORRE, P., 1975. Manuel d'analyse des éléments nutritifs dans l'eau de mer (utilisation de l'autoanalyseur II Technicon), 2^{ème} édition, Université Bretagne Occidentale, 110 pp.
- Van WAMBEKE F., LEFÈVRE, D., PRIEUR, L., SEMPÉRÉ R., BIANCHI, M., OUBELKHEIR, K. & BRUYANT, F., 2004. Distribution of microbial biomass, metabolisms and factors controlling the bacterial production across a geostrophic front (SW Mediterranean Sea). *Marine Ecology Progress Series*, 269:1-15.
- VAULOT, D., 1989. CytoPC: processing software for flow cytometric data. *Signal Noise* 2:8.
- VAULOT, D., PARTENSKY, F., NEVEUX, J., MANTOURA, R. F. C. & LLEWELLYN, C., 1990. Winter presence of prochlorophytes in surface waters of the Northwestern Mediterranean Sea. *Limnology and Oceanography*, 35:1156-1164.
- VAULOT, D. & PARTENSKY, F., 1992. Cell cycle distributions of prochlorophytes in the North Western Mediterranean Sea. *Deep-Sea Research*, 39:727-742.
- VAULOT, D., EIKREM, W., VIPREY, M. & MOREAU, H., 2008. The diversity of small eukaryotic phytoplankton ($\leq 3 \mu\text{m}$) in marine ecosystems. *FEMS Microbiology Reviews*, 32:795-820.
- VIDEAU, C., SOURNIA, A., PRIEUR, L. & FIALA, M., 1994. phytoplankton and primary production characteristics at selected sites in the geostrophic Almeria-Oran front system (SW Mediterranean Sea). *Journal of Marine Systems*, 5:235-250.
- VIPREY, M., GUILLOU, L., FERRÉOL, M. & VAULOT, D., 2008. Wide genetic diversity of picoplanktonic green algae (Chloroplastida) in the Mediterranean Sea uncovered by a phylum-biased PCR approach. *Environmental Microbiology* 10:1804-1822.
- VIUDEZ, A., PINOT, J.-M. & HANEY, R. L., 1998. On the upper layer circulation in the Alboran

- Sea. *Journal of Geophysical Research*, 103:21653-21666.
- WEINBAUER, M.G., BRETTAR, I. & HÖFLE, M.G., 2003. Lysogeny and virus-induced mortality of bacterioplankton in surface, deep and anoxic marine waters. *Limnology and Oceanography*, 48: 1457-1465.
- WEST, N. J. & SCANLAN, D. J., 1999. Niche-partitioning of *Prochlorococcus* populations in a stratified water column in the eastern north Atlantic Ocean. *Applied and Environmental Microbiology*, 65:2585-2591.
- WILHELM, S. W. & SUTTLE, C. A., 1999. Viruses and nutrient cycles in the sea. *Bioscience*, 49:781-788.
- WILMOTTE, A. D., DEMONCEAU, C., GOFFART, A., HECQ, J. H., DEMOULIN, V. & CROSSLEY, A. C., 2002. Molecular and pigment studies of the picophytoplankton in a region of the Southern Ocean (42–54°S, 141–144°E) in March 1998. *Deep-Sea Research II*, 49:3351–3363.
- WINTER, C., KERROS, M. E. & WEINBAUER, M.G., 2009. Seasonal and depth-related dynamics of prokaryotes and viruses in surface and deep waters of the northwestern Mediterranean Sea. *Deep-Sea Research I*, 56: 1972-1982.
- WOMMACK, K. E. & COLWELL, R. R., 2000. Virioplankton: viruses in aquatic ecosystems. *Microbiology and Molecular Biology Reviews*, 64:69-114.
- WORDEN, A. Z. & NOT, F., 2008. Ecology and diversity of picoeukaryotes. In Kirchman, D. L. [ed.], *Microbial Ecology of the Ocean*. Wiley, p. 159-205.
- YOUSARA, F. & GAUDY, R., 2001. Variations of zooplankton in the frontal area of the Alboran Sea (Mediterranean Sea) in winter 1997. *Oceanologica Acta* 24:361-376.
- ZAKARDJIAN, B. & PRIEUR, L., 1998. Biological and chemical signs of upward motions in permanent geostrophic fronts of the Western Mediterranean. *Journal of Geophysical Research*, 103:27849-27866.
- ZAKARDJIAN, B., 1994. Rôle du système advection/diffusion sur la production primaire en zone frontale, Ph.D. thesis, 183pp, Univ. Pierre et Marie Curie, Paris, France.
- ZWIRGLMAIER, K., JARDILLIER, L., OSTROWSKI, M., MAZARD, S., GARCZARECK, L., VAULOT, D., NOT, F., MASSANA, R., ULLOA, O. R. & SCANLAN, D. J., 2008. Global phylogeography of marine *Synechococcus* and *Prochlorococcus* reveals a distinct partitioning of lineages amongst oceanic biomes. *Environmental Microbiology*, 10:147-161.
-